RSC Advances

PAPER

View Article Online
View Journal | View Issue

Cite this: *RSC Adv.*, 2025, **15**, 30360

TiO_2-enhanced fly ash for advanced treatment of persistent organics (POCs) in landfill leachate *via* hybrid ozonation–peroxymonosulfate: degradation efficiency and machine learning modeling

Huu-Tap Van,[a] Thi Cuc Luu,[b] Van Hung Hoang,*[a] Thuy Linh Vi,[c] Thu Huong Nguyen,[c] Trung Kien Hoang,[c] Thi Bich Lien Nguyen,[c] Hoang Nguyen,[b] Thi Hanh Dam,[b] Duc Hien Lu,[b] A. Dia Thao[b] and Lan Huong Nguyen[d]

Landfill leachate is a major environmental concern because of its high content of persistent organic compounds (POCs), which require advanced treatment techniques. This study introduces a novel hybrid ozonation–TiO_2-modified fly ash composite (FA@TiO_2) process enhanced by a peroxymonosulfate (PMS) for POC degradation in landfill leachate. The FA@TiO_2 composite, synthesized *via* the sol–gel method with optimal 20% TiO_2 loading, leverages fly ash's cost-effectiveness and TiO_2's catalytic prowess. Experiments revealed that under optimized conditions—pH 9, PMS dosage of 300 mg L^{-1}, and FA@TiO_2 dosage of 1.00 g L^{-1} – the system achieved 77.90% color removal and 61.59% total organic carbon (TOC) removal after 80 min, with a pseudo-first-order rate constant of 0.0087 min^{-1}. The synergy between FA's metal oxides and TiO_2 nanoparticles enhances reactive oxygen species (ROS) generation, including hydroxyl ($^{\bullet}OH$) and sulfate ($SO_4^{\bullet-}$) radicals, driving POC mineralization. Reusability tests showed the catalyst retained 67.52% color and 40.62% TOC removal efficiencies after five cycles, indicating practical viability despite a performance decline. Radical scavenger studies confirmed OH radicals' dominant role in TOC degradation. This approach offers a sustainable, efficient solution for leachate treatment by repurposing industrial waste and optimizing operational parameters, advancing the application of advanced oxidation processes in environmental remediation. This study evaluates the performance of four machine learning models – Linear Regression, Artificial Neural Network (ANN), Random Forest (RF), and Support Vector Machine (SVM) – in predicting polycyclic organic compound degradation efficiency within the O_3/FA@TiO_2/PMS system, with ANN demonstrating superior accuracy and generalization (R^2 = 0.994, RMSE = 1.18, MAE = 0.956).

Received 10th June 2025
Accepted 16th August 2025

DOI: 10.1039/d5ra04088d

rsc.li/rsc-advances

Introduction

Landfill leachate significantly pollutes water resources due to its high content of persistent organic compounds (POCs), notably humic substances, which can constitute up to 60% of organic matter in aged leachate.[1] These compounds, including humic and fulvic acids, resist biodegradation, altering water pH and color while enhancing the toxicity and mobility of heavy metals through complexation, thus threatening groundwater and surface water quality.[2] Humic substances also exhibit genotoxic effects on aquatic organisms, though they may paradoxically benefit some species in harsh.[3] Their persistence challenges conventional treatment, necessitating advanced methods like low-pH flocculation to reduce chemical oxygen demand and mitigate environmental harm.[4]

A diverse array of technologies has been implemented to treat landfill leachate, effectively addressing its complex mixture of pollutants, which includes persistent organic compounds such as humic substances. Recent studies have underscored the efficacy of biological treatment methods, particularly sequencing batch reactors,[5] alongside membrane technologies like reverse osmosis[6] and physicochemical approaches such as electrocoagulation.[7] Furthermore, advanced oxidation processes (AOPs), which incorporate techniques such as Fenton oxidation, photocatalysis and ozonation, have emerged as robust solutions for the degradation of

[a]*Thai Nguyen University (TNU), Bac Son Road, Phan Dinh Phung Ward, Thai Nguyen, 25000, Vietnam. E-mail: hoangvanhung@tnu.edu.vn*
[b]*Thai Nguyen University – Lao Cai Campus, Lao Cai Ward, Lao Cai, Vietnam*
[c]*Faculty of Natural Resources and Environment, TNU – University of Sciences (TNUS), Phan Dinh Phung Ward, Thai Nguyen, 25000, Vietnam*
[d]*Faculty of Biology and Environment, Ho Chi Minh City University of Industry and Trade (HUIT), 140 Le Trong Tan Street, Tay Thanh Ward, Ho Chi Minh City, Vietnam*

recalcitrant organic compounds.[8] AOPs, particularly ozonation, are particularly effective in decomposing hard-to-degrade organic substances in leachate by generating reactive hydroxyl radicals and ozone molecules, thereby facilitating rapid and efficient degradation that surpasses the performance of conventional treatment methods, significantly diminishing the environmental persistence and toxicity of these contaminants.

Ozonation is a highly effective method for oxidizing organic pollutants in water treatment; however, standalone ozone often yields low efficiency in fully degrading POCs due to its selective reactivity and limited mineralization capacity. To enhance the decomposition of POCs, heterogeneous catalytic ozonation has been widely adopted, leveraging catalysts to promote ozone decomposition into reactive species like hydroxyl radicals, thereby improving degradation efficiency. Recent advancements in the treatment of landfill leachate have highlighted the efficacy of ozonation, particularly when combined with various catalytic agents to enhance the degradation of organic pollutants. Studies have demonstrated that the integration of metallic compounds such as tin tetrachloride ($SnCl_4$) significantly improves the ozonation processes, achieving notable reductions in chemical oxygen demand (COD) and color in stabilized landfill leachate.[9] Furthermore, the application of advanced oxidation processes, including cavitation ozonation, has been shown to effectively target POCs, which is typically resistant to conventional treatment methods.[10] The optimization of ozonation parameters, such as pH and ozone flow rate, is crucial for maximizing pollutant removal efficiency.[11] These findings underscore the potential of catalytic ozonation as a promising approach for addressing the complex challenges associated with organic contaminants in landfill leachate.[12]

Titanium dioxide (TiO_2) nanoparticles have gained recognition as effective heterogeneous catalysts in ozonation processes, attributed to their significant surface area, chemical stability, and ability to enhance the generation of reactive oxygen species (ROS), particularly hydroxyl radicals ($^{\bullet}OH$). When integrated with ozone, TiO_2 nanoparticles facilitate the decomposition of ozone molecules into ROS, thereby enhancing the oxidative degradation of POCs in wastewater, including humic substances and pharmaceuticals. The photocatalytic properties of TiO_2, when combined with ozonation, can improve pollutant mineralization efficiency under ultraviolet (UV) or visible light irradiation, although specific performance comparisons to standalone ozonation methods require further investigation.[13] Recent research has demonstrated that TiO_2 nanoparticles, especially when modified through coating on membranes or metal doping, can achieve notable removal efficiencies for micropollutants, although the specific percentages and treatment durations can vary across different studies. For instance, the synthesis of TiO_2 coupled with other metal oxides, such as CuO and ZnO, has shown improved photocatalytic activity for the degradation of dyes, indicating the potential for enhanced performance in wastewater treatment applications.[14] The synergistic effects of TiO_2 nanoparticles in AOPs highlight their promise as effective catalytic solutions for treating complex wastewater streams.[15]

Fly ash (FA), a byproduct of coal combustion, has gained attention as a cost-effective heterogeneous catalyst in ozonation processes for the degradation of organic compounds in wastewater and landfill leachate. Its high surface area, rich metal oxide content (*e.g.*, SiO_2, Al_2O_3 and Fe_2O_3), and porous structure enable it to enhance ozone decomposition into reactive oxygen species, such as $^{\bullet}OH$, thereby accelerating the breakdown of persistent organic pollutants, including humic substances.[16] Studies show that fly ash, when used as a catalyst, improves the removal efficiency of COD and total organic carbon (TOC) compared to standalone ozonation, offering a sustainable approach by repurposing industrial waste.[17] This application underscores fly ash's potential as an economical and efficient catalyst for advanced wastewater treatment.

Peroxymonosulfate (PMS) is increasingly recognized as a promising catalytic agent in advanced oxidation processes, particularly in ozonation. Its ability to generate highly reactive species, such as sulfate radicals ($SO_4^{\bullet-}$) and $^{\bullet}OH$, enhances the degradation efficiency of organic pollutants.[18] When integrated into ozonation, PMS acts as a synergistic activator, promoting the decomposition of ozone (O_3) and facilitating the formation of additional reactive oxygen species (ROS). This combined approach not only improves the oxidation capacity but also extends the applicability of ozonation to a wider range of contaminants, making PMS a valuable component in advanced water treatment technologies.

Although TiO_2 nanoparticles and FA have been individually investigated as catalysts for ozonation to degrade POCs in wastewater and landfill leachate, the development of a novel composite material (FA@TiO_2) combined with PMS activation for enhancing ozone-driven POC degradation in landfill leachate has not been extensively explored. TiO_2 is known for its high catalytic activity and stability, while FA offers cost-effectiveness and a porous structure enriched with metal oxides. However, research integrating these materials into a composite catalyst remains limited. The novelty of this study lies in the synthesis of the FA@TiO_2 composite as a synergistic catalyst, coupled with PMS activation, to leverage the complementary properties of both materials for improved POC degradation efficiency in landfill leachate. This approach not only repurposes industrial waste but also addresses the challenges associated with treating recalcitrant organic pollutants, offering a sustainable and innovative solution for leachate management.

The main objective of this research is to synthesize a composite material (FA@TiO_2) by combining FA and TiO_2 nanoparticles and to apply it in hybrid ozonation process (O_3/FA@TiO_2/PMS) for the degradation of POCs in landfill leachate. The study will systematically evaluate the influence of key operational parameters, including the TiO_2-to-FA ratio, leachate pH, PMS dosage, catalyst dosage, coexisting anions, and the reusability potential of the composite, on the degradation efficiency. Furthermore, the research aims to elucidate the underlying mechanisms of POC decomposition through catalytic ozonation, providing insights into the synergistic effects of the FA@TiO_2 composite and its practical applicability in sustainable leachate treatment. This work seeks to advance the understanding of composite catalysts and their role in

enhancing advanced oxidation processes for environmental remediation.

Additionally, to optimize the effectiveness of environmental treatment applications, the research team constructed machine learning models to forecast treatment efficiency across diverse chemical formulations. Drawing from established applications of machine learning in chemistry and environmental engineering,[19] four prevalent models – Artificial Neural Network (ANN), Random Forest (RF), Support Vector Machine (SVM), and Linear Regression (LR) – were selected to develop predictive models based on experimental data from the project. This methodology aims to enhance the feasibility of practical implementation and improve real-world applicability.

Materials and methods

Chemicals

CH_3CH_2OH 99%, tetraclorua $TiCl_4$ 99.99%, sodium hydroxide (NaOH) and sulfuric acid (H_2SO_4) obtained from Merck at analytical grade and used as received without additional purification.

The landfill leachate utilized in this study was derived from domestic solid waste, which was incubated in sealed 30 liter plastic containers for a duration of six months. During the incubation period, no additional water was introduced. Following incubation, the leachate was extracted *via* suction and subsequently diluted five-fold with water to simulate realistic environmental conditions. This dilution step was necessary to adjust the leachate concentration to levels more representative of those encountered in natural settings.

Materials

FA@TiO_2 synthesis. The synthesis of FA@TiO_2 composite nanomaterials with varying TiO_2 ratios (10%, 20% and 30%) was conducted using the sol–gel method. The procedure encompasses several specific steps as follows: initially, to prepare the hydrolysis solution, 50 mL of absolute ethanol (99.99% purity) was mixed with 1.8 mL of ultrapure water in the first beaker. The use of absolute ethanol is crucial for controlling the reaction by ensuring the absence of excess water, while ultrapure water initiates the hydrolysis of the titanium precursor. Subsequently, in the preparation of the TiO_2 precursor solution, 35 mL of tetrabutyl titanate (containing approximately 1.419 g of Ti), 90 mL of absolute ethanol, and 10 mL of acetylacetone were combined in the second beaker. Tetrabutyl titanate ($Ti(OC_4H_9)_4$) serves as the primary precursor for TiO_2 formation, while acetylacetone acts as a chelating agent, regulating the hydrolysis rate, preventing rapid precipitation, and facilitating the formation of uniform TiO_2 nanoparticles. Following this, during the hydrolysis and pH adjustment phase, the solution from the first beaker was gradually added to the second beaker, and the pH was adjusted to 5 using 67% nitric acid (HNO_3). This mild acidic condition optimizes the hydrolysis and condensation reactions, promoting the formation of TiO_2 particles. The mixture was then stirred and a surfactant was added: vigorous stirring at room temperature for one hour ensured homogeneity, after which 2 g of polyethylene glycol (PEG) was incorporated as a surfactant to control particle size and prevent agglomeration. The mixture continued to be stirred at 50 °C for one hour, yielding a transparent yellow solution, indicative of a stable sol. To form the composite, fly ash was added in appropriate amounts to achieve the desired TiO_2 ratios: 12.42 g of FA for 10% TiO_2, 11.04 g for 20%, and 9.66 g for 30%. The mixture was continuously stirred for one hour to ensure uniform distribution of the fly ash. Subsequently, the mixture was aged by allowing it to stand for 24 hours to complete the sol–gel process and ensure the adhesion of TiO_2 particles to the surface of the fly ash. The drying phase involved evaporating the mixture at 80 °C in a water bath until nearly dry, followed by complete drying at 80 °C to remove the solvent and promote gelation. Finally, the solid residue was calcined at 500 °C for 2 hours to eliminate organic components and facilitate the formation of crystalline TiO_2.

Experiment

The degradation of POCs from landfill leachate was conducted using a batch process. Ozone was generated utilizing an ozone generator (Vietzone 20P, Vietzone Ozone Generator Joint Stock Company, Vietnam), which achieved a maximum inlet ozone (O_3) output of 5.0 g h^{-1} at a flow rate of 15 mL min^{-1}, with an effective operational capacity of 4.149 g h^{-1}. Pure oxygen, sourced from a cylinder, served as the feed gas for the generator. The freshly produced ozone was introduced into a resin reactor (height = 700 mm, inner diameter = 60 mm) *via* a diffuser positioned at the base of the reactor.

The experiments were designed to evaluate the influence of key parameters on the efficiency of POCs treatment from leachate using an ozonation system combined with the FA@TiO_2 catalyst and the presence of PMS. Specifically, the study examined the effect of the TiO_2 composite ratio (10–30%) within the FA@TiO_2 framework. Samples of FA@TiO_2 with varying TiO_2 ratios (10%, 20% and 30%) were utilized to ascertain the optimal proportion that yields the highest POCs degradation efficiency. The impact of pH (3–11) was also assessed, with the pH of the leachate being adjusted from 3 to 11 to identify the optimal value for the treatment process. Moreover, the PMS (200–400 mg L^{-1}) and FA@TiO_2 (0.25–1.5 g L^{-1}) was varied to determine the optimal amount for the treatment process. The reusability of the FA@TiO_2 catalyst was evaluated over five cycles to assess its durability and the ability to maintain treatment efficiency, which is a critical factor for evaluating the practicality of the technology in real-world applications.

All experiments were conducted in a reactor containing 500 mL of leachate, with the ozonation process occurring in cycles of 5 minutes, culminating in a total treatment duration of 80 minutes.

Machine learning modeling and hyperparameter optimization

To enhance the precision of predictive models for O_3/FA@TiO_2/PMS – mediated degradation of persistent organic compounds (POCs), a systematic model development approach was

implemented using Rstudio. Prior to model construction, the selection of an appropriate evaluation metric and identification of critical input features were deemed essential. In this investigation, the removal efficiency of POCs was adopted as the primary performance metric, with initial pH, catalyst dosage, PMS concentration and reaction time designated as the four principal descriptors. While reliance on a single evaluation metric may introduce minor inaccuracies, this study aimed to provide a preliminary assessment of degradation performance across diverse reaction conditions. This methodology offers the potential to reduce experimental resource demands, thereby improving efficiency and cost-effectiveness.

To predict the degradation efficiency of persistent organic compounds (POCs) in the O_3/FA@TiO_2/PMS system, four machine learning models – Linear Regression (LR), Artificial Neural Network (ANN), Random Forest (RF), and Support Vector Machine (SVM) – were implemented using R software (version 4.3.1, R Core Team, 2024). The dataset (128 samples) included four input features (pH, reaction time, PMS dosage, catalyst dosage) and the target variable (removal efficiency, %). Data was split into 80% training (102 samples) and 20% testing (26 samples) sets[20] using stratified sampling (caret::createDataPartition, seed = 42). Features were standardized using caret::preProcess (centered and scaled for LR, RF, ANN; scaled to [0, 1] for SVM).

Hyperparameter optimization: Linear Regression (LR): implemented using ordinary least squares (lm function) without hyperparameter tuning. Artificial Neural Network (ANN): a single-hidden-layer neural network was trained using caret::nnet. Grid search was conducted over hidden layer sizes (2–20) with decay = 0.01 and maxit = 50 000. The optimal configuration was 4 hidden nodes. Random Forest (RF): trained using caret::rf with a tune grid search (10-fold cross-validation) over mtry (1–4), min.node.size (1, 2, 4), maxdepth (10, 20, 30, unlimited), and ntree (100, 500, 1000). The optimal parameters were mtry = 2, ntree = 500, nodesize = 5, maxnodes = NULL. Support Vector Machine (SVM): implemented using e1071 with random search (10-fold cross-validation) over kernel (linear, polynomial, radial), C (0.01, 0.1, 1, 10), gamma (0.001, 0.01, 0.1), and degree (1, 2, 3). The optimal configuration was kernel = polynomial, C = 10, degree = 3, gamma = 0.1, epsilon = 0.1.

Model performance was evaluated using R^2, RMSE, and MAE. A fixed seed (42) ensured reproducibility. The complete R code for data preprocessing, hyperparameter tuning, model training, and visualization is available in the SI section *via* a GitHub repository.

The performance of each algorithm was evaluated using R^2, RMSE, and MAE. The R^2 metric quantifies the proportion of variance in the dependent variable explained by the independent variables, with values approaching 1 indicating superior model fit. RMSE measures the square root of the average squared differences between predicted and actual values, providing insight into prediction accuracy. Lower RMSE values signify enhanced precision and improved capture of underlying data patterns. MAE, defined as the average of absolute differences between predicted and observed values, offers a complementary measure of model accuracy, emphasizing the magnitude of errors without squaring, thus providing a linear representation of prediction deviations. The equations for these metrics are presented below:[20]

$$R^2 = 1 - \frac{\sum_{i=1}^{n}\left(y_i - \hat{y}_i\right)^2}{\sum_{i=1}^{n}\left(y_i - \bar{y}\right)^2} \quad (1)$$

where y_i is the actual value, $\hat{y}_i$ is the predicted value, $\bar{y}$ is the mean of observed values, and n is the number of observations.

$$\mathrm{RMSE} = \sqrt{\frac{1}{n}\sum_{i=1}^{n}\left(y_i - \hat{y}_i\right)^2} \quad (2)$$

$$\mathrm{MAE} = \frac{1}{n}\sum_{i=1}^{n}\left|y_i - \hat{y}_i\right| \quad (3)$$

These metrics collectively facilitate a comprehensive evaluation of model performance, ensuring reliable predictions for POCs degradation under varying experimental conditions.[21]

Measurement

The optical absorbance of the aqueous phase was measured with a UV-Vis spectrophotometer (Shimadzu, model Z2000, Japan) at an absorption wavelength of 520 nm. Simultaneously, TOC concentrations were analyzed using a Multi TOC/TN analyzer (Multi N/C 3100, Analytik Jena). The solution's pH was modified by adding 0.1 M HCl or 0.1 M NaOH, with real-time pH tracking performed *via* a calibrated pH meter (HANNA, model HI 2211-02, Romania). Morphological and elemental composition features of the FA@TiO_2 composite were characterized using scanning electron microscopy (SEM) coupled with energy-dispersive X-ray spectroscopy (EDX) at 2.0 kV acceleration voltage under varying magnifications (JSM-IT200, InTouchScope). Furthermore, the crystalline phase composition of the slag particles was determined by X-ray diffraction (XRD) with a Siemens D5005 diffractometer equipped with CuKα radiation (λ = 1.5417 Å).

Results and discussion

Effect of composite ratio for FA@TiO_2 synthesis on POCs removal by catalytic ozonation

The experimental investigation presented in Fig. 1 demonstrates that the FA@TiO_2 composite ratio plays a critical role in enhancing the performance of catalytic ozonation for the removal of POCs from landfill leachate. Under the experimental conditions – an initial TOC concentration of 371 mg L^{-1}, pH 7.7, catalyst dosage of 0.5 g L^{-1}, PMS dosage of 300 mg L^{-1} and reaction times varying from 0 to 80 min – five operational scenarios were evaluated: O_3 alone, O_3/FA@TiO_2 20%, O_3/FA@TiO_2 10% with PMS, O_3/FA@TiO_2 20% with PMS and O_3/FA@TiO_2 30% with PMS.

Regarding color removal (Fig. 1a), all systems exhibited a time-dependent increase in efficacy. At 80 min, the O_3/FA@TiO_2 30%/PMS configuration recorded the maximum color

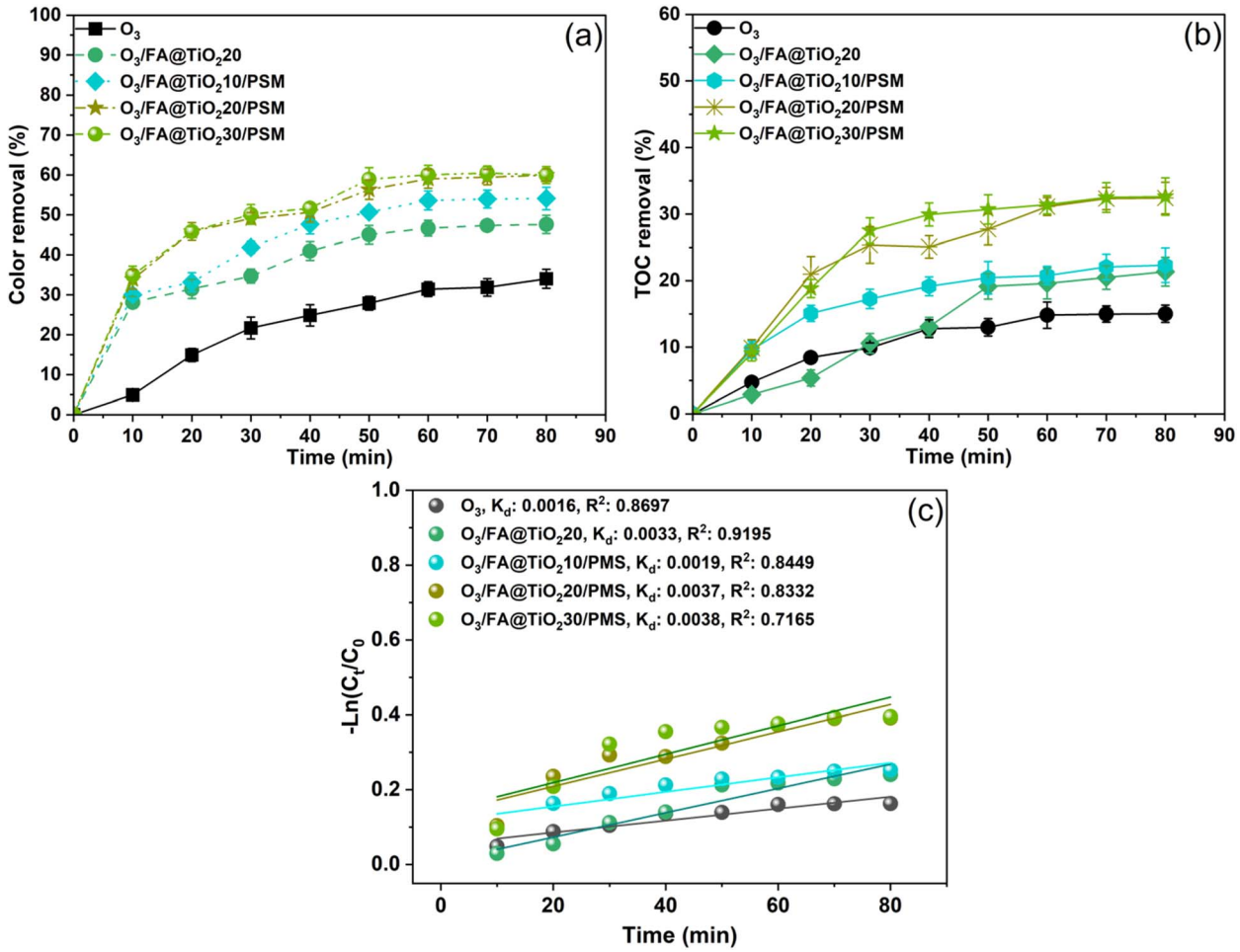

Fig. 1 Effect of various composite ratios between TiO_2 and FA as catalytic for ozonation processes to removal of POCs from landfill leachate (a) color; (b) TOC and (c) pseudo-first-order rate constants at initial TOC concentration of 371 mg L^{-1}; pH of 7.7; catalyst dosage of 0.5 g L^{-1}, PMS dosage of 300 mg L^{-1} and contact time of 0–80 min.

removal efficiency of 59.96%. Notably, the O_3/FA@TiO_2 20%/PMS system reached the same efficiency value (59.96%), while lower efficiencies were observed for O_3/FA@TiO_2 10%/PMS (54.09%), O_3/FA@TiO_2 20% without PMS (47.59%), and O_3 alone (40.40%). For TOC removal (Fig. 1b), a similar pattern was evident; the O_3/FA@TiO_2 30%/PMS system yielded a TOC removal efficiency of 32.62% at 80 min, closely followed by the 20% TiO_2 system at 32.41%. The systems lacking PMS showed lower removal efficiencies, with O_3/FA@TiO_2 20% achieving 21.35% and O_3 alone only 15.07%.

The observed performance is closely linked to the generation of ROS on the catalyst surface. Enhanced TiO_2 loading increases the density of active sites, thereby promoting the decomposition of ozone into $^{\bullet}OH$ and activating PMS to generate sulfate radicals ($SO_4^{\bullet-}$).[22,23] Although the 30% TiO_2 composite produced slightly higher pseudo-first-order reaction kinetics (k_d = 0.0038 min^{-1}, R^2 = 0.7165) compared to the 20% composite (k_d = 0.0037 min^{-1}, R^2 = 0.8332) as shown in Fig. 1c, the marginal differences in both TOC and color removal efficiencies indicate that the additional catalyst does not translate into substantially improved performance. Excess TiO_2 may promote particle agglomeration, thereby reducing the effective surface area available for ROS generation, as reported in recent advances in TiO_2-based advanced oxidation processes.[23,24]

The near equivalence in performance between the O_3/FA@TiO_2 20%/PMS and O_3/FA@TiO_2 30%/PMS systems suggests that a 20% TiO_2 ratio is optimal. This condition not only delivers comparable degradation efficiency (with 32.41% TOC removal and 59.96% color removal at 80 minutes) but does so with lower catalyst consumption, which is more economically viable for large-scale applications. Moreover, the optimal contact time was determined to be 60 min, achieving 31.12% TOC removal and 59.01% color removal, beyond which the removal efficiencies increased negligibly. These observations are consistent with kinetic modeling studies that highlight the importance of balancing catalyst loading and reaction time to maximize pollutant degradation while minimizing operational costs (Kumari & Pulimi, 2023).[24]

Therefore, a 20% TiO_2 composite ratio in the catalyst blend provides an optimum balance between catalyst efficiency and cost-effectiveness. The synergistic activation of ozone and PMS under these conditions fosters effective ROS generation for the

degradation of organic pollutants, while the kinetic parameters affirm that further increases in TiO_2 loading do not translate into proportional gains in removal efficiency. Such findings underscore the critical role of catalyst optimization in advanced oxidation processes for wastewater treatment.

Characteristics of FA@TiO_2 catalyst

The scanning electron microscopy (SEM) images presented in Fig. 2 offer comprehensive morphological characterization of FA and its composite with titanium dioxide (FA@TiO_2). The SEM image labeled (Fig. 2a1) illustrates the surface morphology of pristine FA, which reveals a heterogeneous structure comprising irregularly shaped particles that exhibit a porous and rough texture. The particle sizes appear to vary, typically on the order of micrometers, as indicated by the accompanying 1.0 μm scale bar. This porosity and irregularity are characteristic of fly ash, which is predominantly composed of aluminosilicate spheres along with unburned carbon residues resulting from the combustion of coal.[25]

In contrast, the SEM image designated as (Fig. 2b1) for FA@TiO_2 demonstrates a significant alteration in surface morphology compared to the pristine FA. The composite material manifests a more uniform particle distribution, evident in the presence of finer, more spherical features layered upon the foundational FA structure. This observation suggests that the deposition or coating of TiO_2 onto the FA surface has been successfully achieved. The rough texture of FA is found to be partially alleviated, likely attributable to the formation of a TiO_2 layer, which is recognized for exhibiting a smoother and more crystalline morphology, particularly under controlled synthesis conditions.[26] Notably, the retention of the 1.0 μm scale bar implies that the overall particle size distribution remains akin to that of pristine FA, indicating that the TiO_2 modification does not result in a substantial alteration of the macroscopic dimensions. Rather, it enhances the surface characteristics, potentially influencing the material's application in various industrial processes.

The energy dispersive X-ray spectroscopy (EDX) analyses and their corresponding elemental compositions offer quantitative insights into the chemical makeup of FA and its composite with titanium dioxide (FA@TiO_2), providing strong evidence for the successful incorporation of TiO_2 into the composite material. The EDX spectrum for pristine FA (designated as Fig. 2a2) reveals a significant predominance of carbon (C) at 35.29 wt% (46.21 atomic%), and oxygen (O) at 15.49 wt% (15.95 atomic%), which are indicative of the organic and oxide components prevalent in FA. Moreover, considerable quantities of silicon (Si,

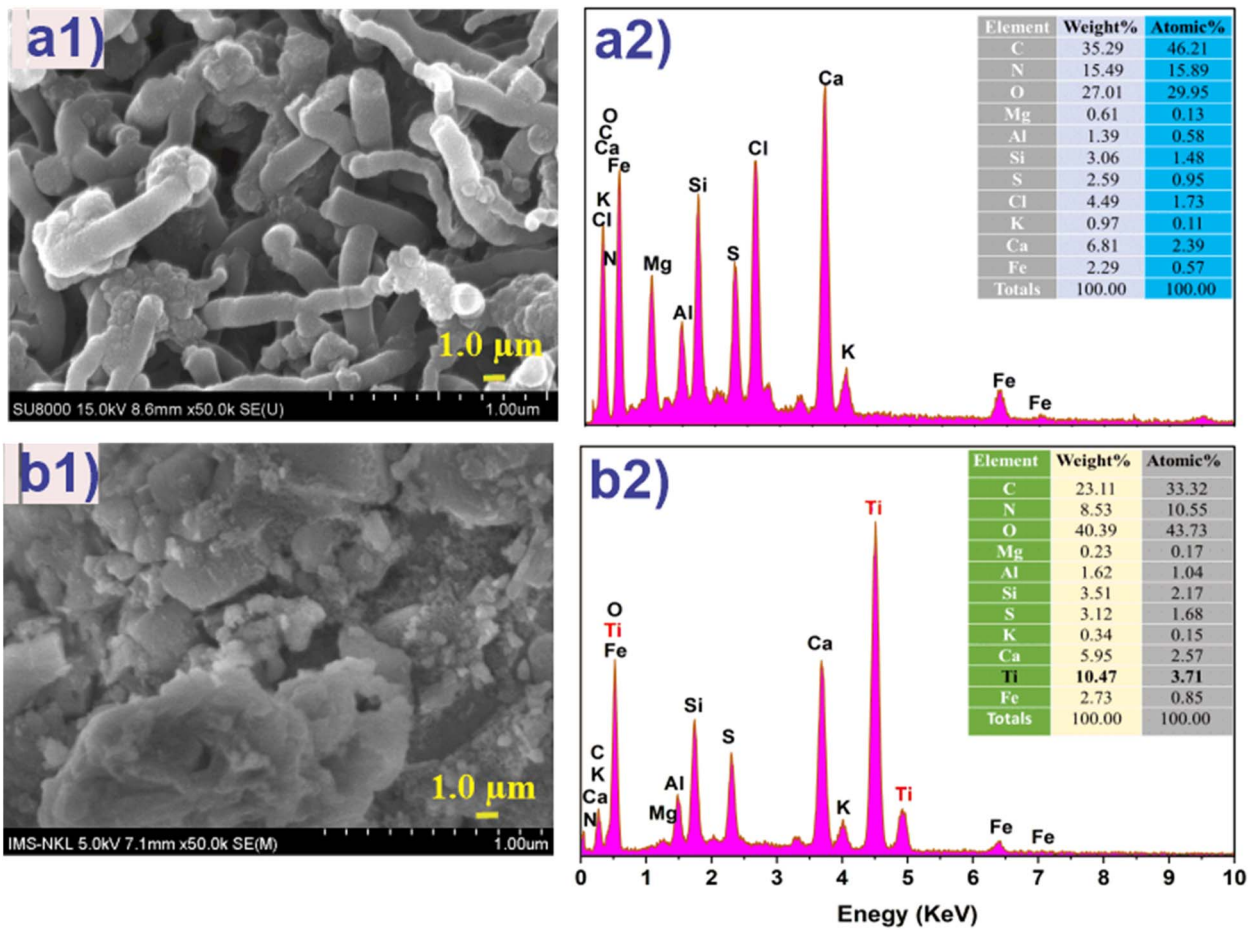

Fig. 2 SEM images of FA (a1), FA@TiO_2 (b1) and EDX spectrum of FA (a2) and FA@ TiO_2 (b2).

3.06 wt%, 1.48 atomic%) and iron (Fe, 2.29 wt%, 0.57 atomic%) are detected, reflecting the well-documented aluminosilicate and iron oxide phases that are characteristic of conventional FA compositions.[25] Trace elements, including calcium (Ca, 6.81 wt%, 2.39 atomic%), magnesium (Mg, 1.39 wt%, 0.58 atomic%), aluminum (Al, 0.61 wt%, 0.13 atomic%), potassium (K, 0.97 wt%, 0.11 atomic%), and chlorine (Cl, 4.49 wt%, 1.73 atomic%), are also present in minor concentrations, suggesting a diverse mineralogical makeup of the fly ash material.

In contrast, the EDX spectrum for the FA@TiO_2 composite (designated as Fig. 2b2) reveals a significant alteration in elemental composition, affirming the successful functionalization with TiO_2. The most prominent observation is the emergence of titanium (Ti, 5.95 wt%, 2.57 atomic%), which is not present in pristine FA, thereby confirming the incorporation of TiO_2 into the composite structure. Concurrently, the carbon content decreases to 23.11 wt% (31.32 atomic%), while the oxygen content increases to 40.39 wt% (43.73 atomic%), likely as a result of the oxide nature of TiO_2. The levels of Si (3.12 wt%, 2.17 atomic%) and Fe (2.73 wt%, 0.85 atomic%) remain largely consistent with those observed in pristine FA, suggesting that the fundamental structure of the FA is preserved despite the addition of TiO_2. Notably, the calcium content increases to 10.47 wt% (3.71 atomic%), which may be attributed to chemical interactions between Ca-rich phases present in FA and the TiO_2 coating process. Also, trace elements such as Al, Mg, K, and sulfur (S) remain detectable, although their concentrations are notably reduced, indicating minimal interference resulting from the composite formation.

The X-ray diffraction (XRD) analysis FA, TiO_2 nanoparticles, and the FA@TiO_2 composite, as presented in Fig. 3, offers critical insights into their crystallographic structures, phase compositions, and the successful incorporation of TiO_2 nanoparticles into the FA matrix. The diffraction patterns, plotted as intensity against the diffraction angle 2θ (ranging from 10° to 80°), reveal distinct features for each sample. The FA pattern is dominated by a broad amorphous hump centered at $2\theta \approx 20$–30°, indicative of its glassy phase, with sharp crystalline peaks at $2\theta \approx 26.6°$ ((002) plane of quartz, SiO_2, JCPDS card no. 46-1045),[27] and minor peaks at $2\theta \approx 20.8°$, 36.5°, and 50.1° (attributed to mullite or aluminosilicates, *e.g.*, (110), (210), and (331) planes of $Al_6Si_2O_{13}$, JCPDS card no. 15-0776), reflecting limited crystallinity within its heterogeneous composition. In contrast, the TiO_2 nanoparticle pattern exhibits sharp peaks at $2\theta \approx 25.3°$ ((101) plane), 37.8° ((004) plane), 48.0° ((200) plane), 54.0° ((105) plane), and 62.7° ((204) plane), consistent with the anatase phase (JCPDS card no. 21-1272),[28] indicating high crystallinity and phase purity with no rutile phase (*e.g.*, $2\theta \approx 27.4°$ absent). The FA@TiO_2 composite pattern integrates these features, retaining the amorphous hump and FA peaks (*e.g.*, $2\theta \approx 26.6°$ for quartz) alongside TiO_2 peaks (*e.g.*, $2\theta \approx 25.3°$), confirming successful compositing. Quantitative analysis reveals a slight reduction in FA peak intensity and a broadening of TiO_2 peaks (from 0.4–0.6° to 0.5–0.7°), suggesting TiO_2 loading of approximately 20–30 wt% and crystallite sizes of 15–20 nm, indicating minimal agglomeration. The absence of new peaks or shifts in TiO_2 peak positions confirms phase stability and interfacial interaction without chemical reaction, positioning the composite as a promising material for photocatalysis due to the retained anatase properties and supportive FA matrix. Further optimization and performance studies are warranted to enhance its applicability.

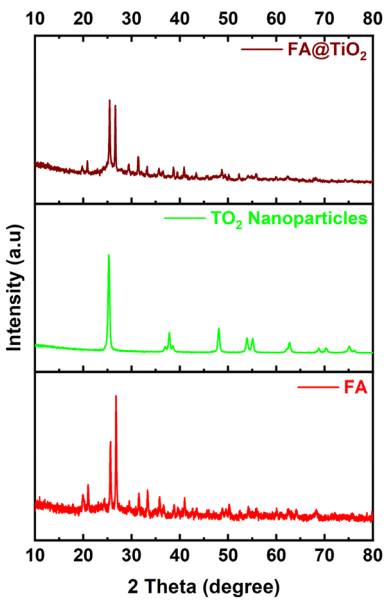

Fig. 3 XRD patterns of FA, TiO_2 nanoparticles and FA@TiO_2 composite.

Effect of leachate pH

The influence of pH on the efficiency of an O_3/FA@TiO_2/PMS system for the removal of POCs from landfill leachate was systematically investigated under controlled experimental conditions (initial TOC of 371 mg L^{-1}, natural pH 7.7, catalyst dosage of 0.5 g L^{-1}, PMS dosage of 300 mg L^{-1}, and contact times spanning 0–80 min) using FA@TiO_2 composite catalyst containing 20% TiO_2. Three key performance metrics were monitored: color removal efficiency, TOC removal efficiency and the pseudo-first-order rate constants (k_d).

The experimental data indicate that both color and TOC removal efficiencies are significantly influenced by the leachate pH. Color removal efficiency increased from 35.44% at pH 3 to 42.57% at pH 5, 50.76% at pH 7, 61.86% at pH 9 and achieved 63.78% at pH 11 after 80 min. This trend clearly demonstrates that higher pH values enhance the decolorization process; however, the marginal 1.92% incremental improvement between pH 9 and pH 11 suggests that the reaction rate approaches a saturation limit beyond pH 9.[29] A nearly identical trend was observed for TOC removal, which increased from 16.07% at pH 3 to 19.81% at pH 5, 27.48% at pH 7, 38.19% at pH 9 and reached 40.11% at pH 11 after 80 minutes. These outcomes corroborate that the organic mineralization process becomes markedly enhanced between pH 7 and pH 9, thus implying that the benefits of further increasing the pH are marginal.[30]

The underlying mechanism for the enhanced removal efficiencies at higher pH appears to be the increased generation of

ROS, primarily $^{\bullet}OH$ and $SO_4^{\bullet-}$. Under alkaline conditions, the activation of PMS by the FA@TiO_2 catalyst is more efficient; PMS is more readily decomposed into ROS, which in turn promote the mineralization of organic pollutants into CO_2 and H_2O. Furthermore, the deprotonation of the organic compounds under these conditions facilitates electrophilic attack by the radicals. In contrast, at lower pH, the system suffers from reduced PMS stability and enhanced scavenging effects by hydrogen ions, leading to lower radical generation.[29] This mechanistic insight is consistent with the literature, which emphasizes that alkaline media favor the formation of oxidants critical for AOPs.

Complementary kinetic analysis using the pseudo-first-order model revealed that the k_d values for TOC removal increased with pH, being 0.0020 min^{-1} at pH 3, 0.0026 min^{-1} at pH 5, 0.0030 min^{-1} at pH 7, 0.0043 min^{-1} at pH 9, and 0.0046 min^{-1} at pH 11. The relatively modest increase in the rate constant beyond pH 9 (an increment of only 0.0003 min^{-1} between pH 9 and pH 11) further supports the observation that the oxidative degradation process reaches a plateau at alkaline conditions. The high k_d values at elevated pH levels are attributed to an accelerated generation of ROS, which expedites the degradation kinetics and corroborates the suitability of the pseudo-first-order model for describing the process.[30]

From a practical standpoint, although operating at pH 11 results in the highest removal efficiencies and reaction rate, the benefits over pH 9 are marginal. Operating at pH 9, which is closer to the natural pH of the leachate (7.7), minimizes the need for extensive pH adjustment, thereby reducing operational costs and mitigating potential secondary issues such as precipitate formation or subsequent pH neutralization requirements. This trade-off between optimal performance and practical feasibility aligns with current perspectives in the treatment of landfill leachate using AOPs (Fig. 4).

Effect of PMS dosage

The catalytic ozonation process using the FA@TiO_2, in the presence of PMS as an oxidant, was comprehensively examined for its efficacy in degrading organic pollutants in landfill

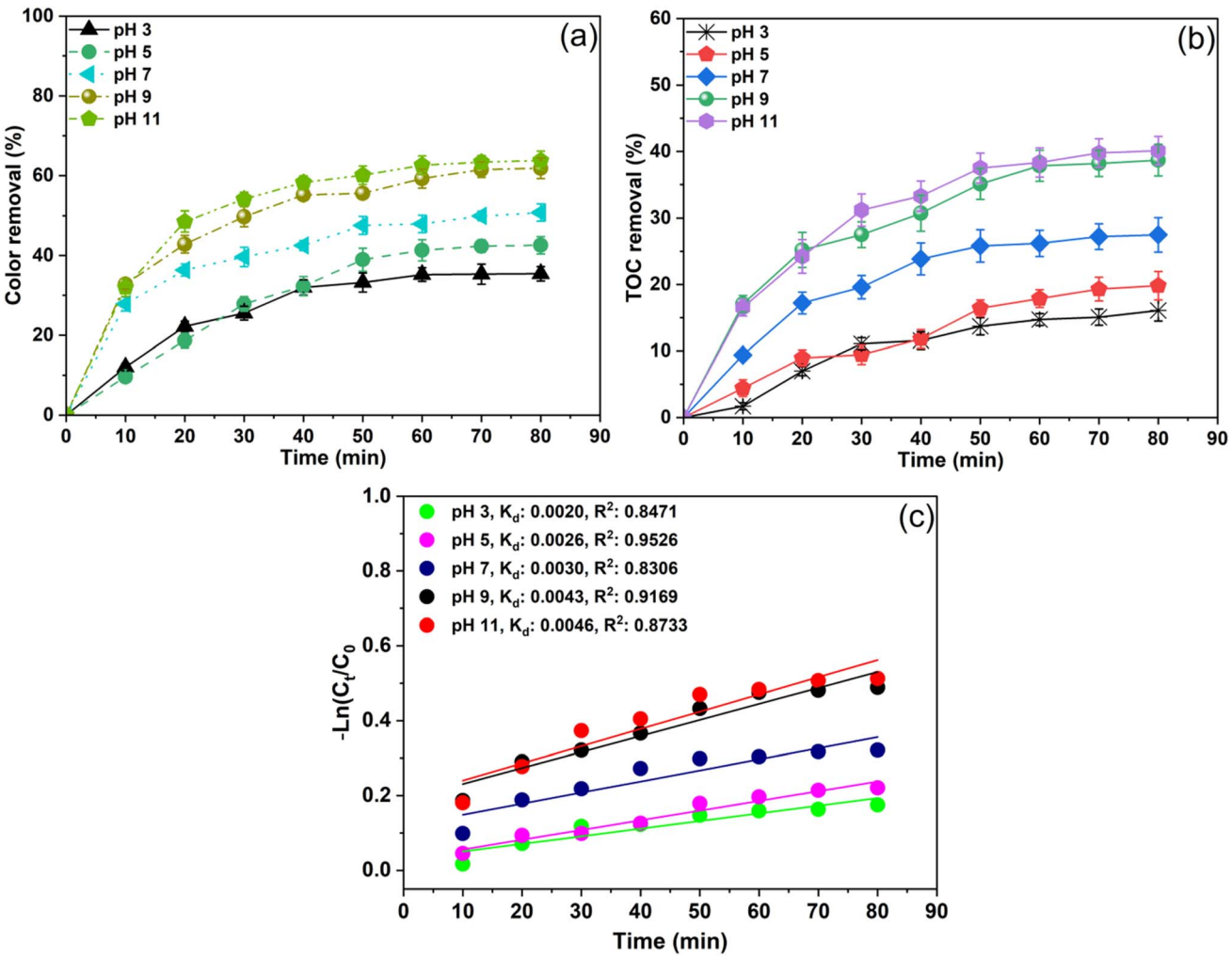

Fig. 4 Influence of pH on removal of POCs from landfill leachate (a) color; (b) TOC and (c) pseudo-first-order rate constants by O_3/FA@TiO_2/PMS system at initial TOC concentration of 371 mg L^{-1}; pH from 3 to 11; catalyst dosage of 0.5 g L^{-1}, PMS dosage of 300 mg L^{-1} and contact time of 0–80 min.

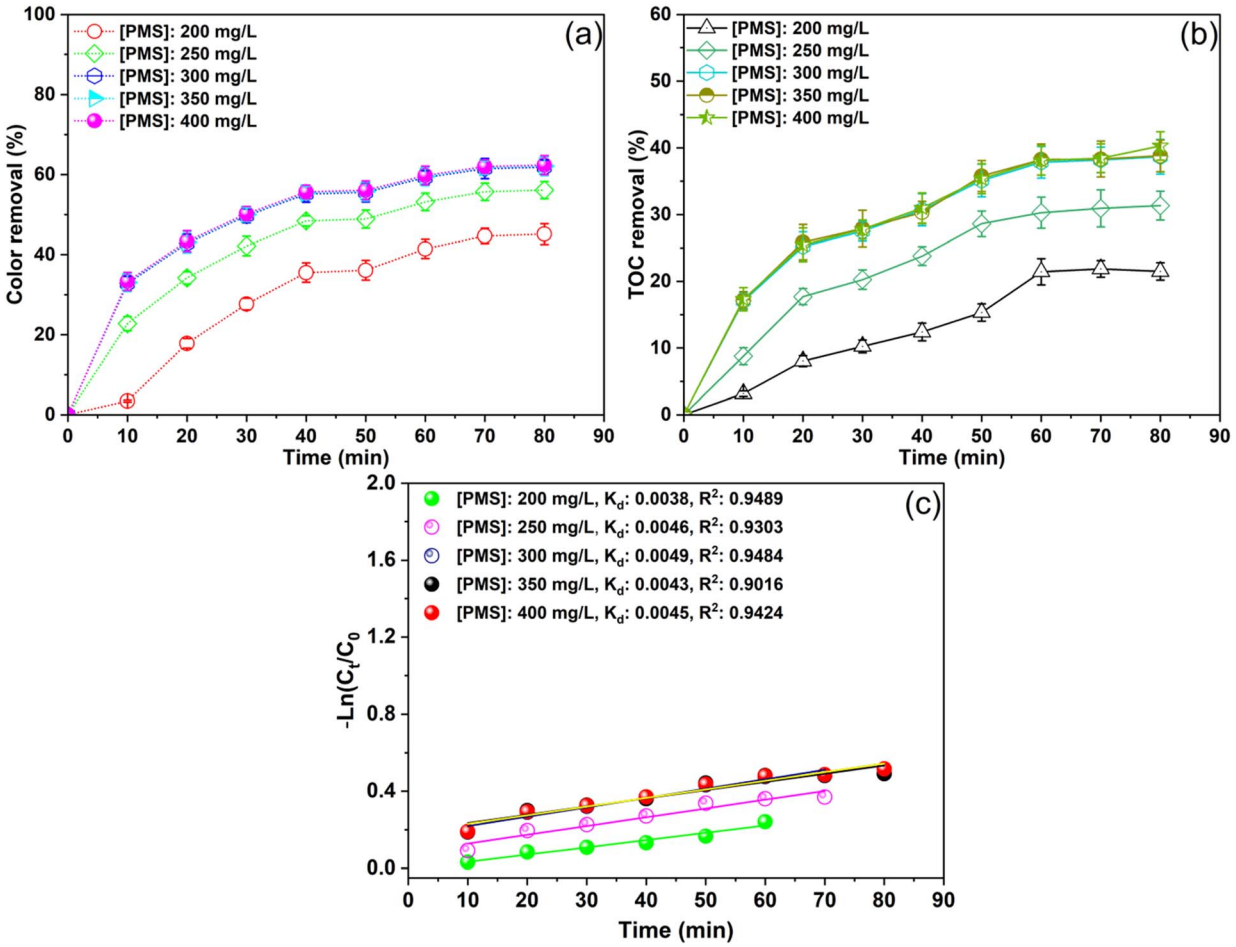

Fig. 5 Influence of PMS dosage on removal of POCs from landfill leachate (a) color; (b) TOC and (c) pseudo-first-order rate constants by O_3/FA@TiO_2/PMS system at initial TOC concentration of 371 mg L^{-1}; pH of 9.0; catalyst dosage of 0.5 g L^{-1}; PMS dosage from 200 to 400 mg L^{-1} and contact time of 0–80 min.

leachate. The study systematically evaluated three key performance indicators: color removal efficiency (%), TOC removal efficiency (%) and TOC degradation kinetics, as depicted in Fig. 5a, b and c, respectively. Similar to AOP approaches, the combination of catalytic ozonation and PMS activation offers a promising pathway for generating ROS, such as $SO_4^{\bullet-}$ and $^{\bullet}OH$, which play central roles in oxidative degradation.[31]

Fig. 5a presents the temporal evolution of color removal efficiency under varying PMS dosages (200, 250, 300, 350 and 400 mg L^{-1}). At a dosage of 200 mg L^{-1}, the color removal reached 45.13% after 80 min; however, an increase in the PMS dosage enhanced this efficiency to 56.12%, 61.86%, 62.12% and 62.38% at 250, 300, 350 and 400 mg L^{-1}, respectively. The pronounced improvement between 200 and 300 mg L^{-1} underscores the critical role of PMS in augmenting the generation of ROS that facilitate the oxidation of chromophoric groups (*e.g.*, humic substances, aromatic compounds,…). Above 300 mg L^{-1}, the marginal increase evidenced by differences of only 0.26% and 0.52% at 350 and 400 mg L^{-1}, respectively, suggests a saturation phenomenon. This may be attributable to the self-scavenging reactions among the generated radicals, as excessive radical concentrations can lead to competitive recombination processes that diminish net oxidative power.[32,33]

In parallel, the TOC removal efficiency, which reflects the extent of mineralization of organic compounds, showed a similar saturation trend (Fig. 5b). Initial measurements indicated TOC removal efficiencies of 21.50% at 200 mg L^{-1}, progressively increasing to 31.34% at 250 mg L^{-1} and 38.68% at 300 mg L^{-1}. Beyond this optimal dosage, the enhancement becomes subdued with efficiencies of 38.81% and 40.29% at 350 mg L^{-1} and 400 mg L^{-1}, respectively. This plateau is indicative of the catalytic system reaching a limit in its capacity to oxidize residual organic compounds; the majority of more readily oxidizable substances are mineralized by 300 mg L^{-1}, leaving behind recalcitrant organic fractions that are less susceptible to further oxidation.[34,35] The observed plateau also highlights that excessive PMS consumption can incur unnecessary chemical costs and potential secondary environmental impacts.

The kinetic study presented in Fig. 5c confirmed that the degradation of TOC adheres to a pseudo-first-order kinetic model, with the rate of reaction (expressed as $-\ln(C/C_0)$ *versus* time) yielding high correlation coefficients (R^2 values ranging

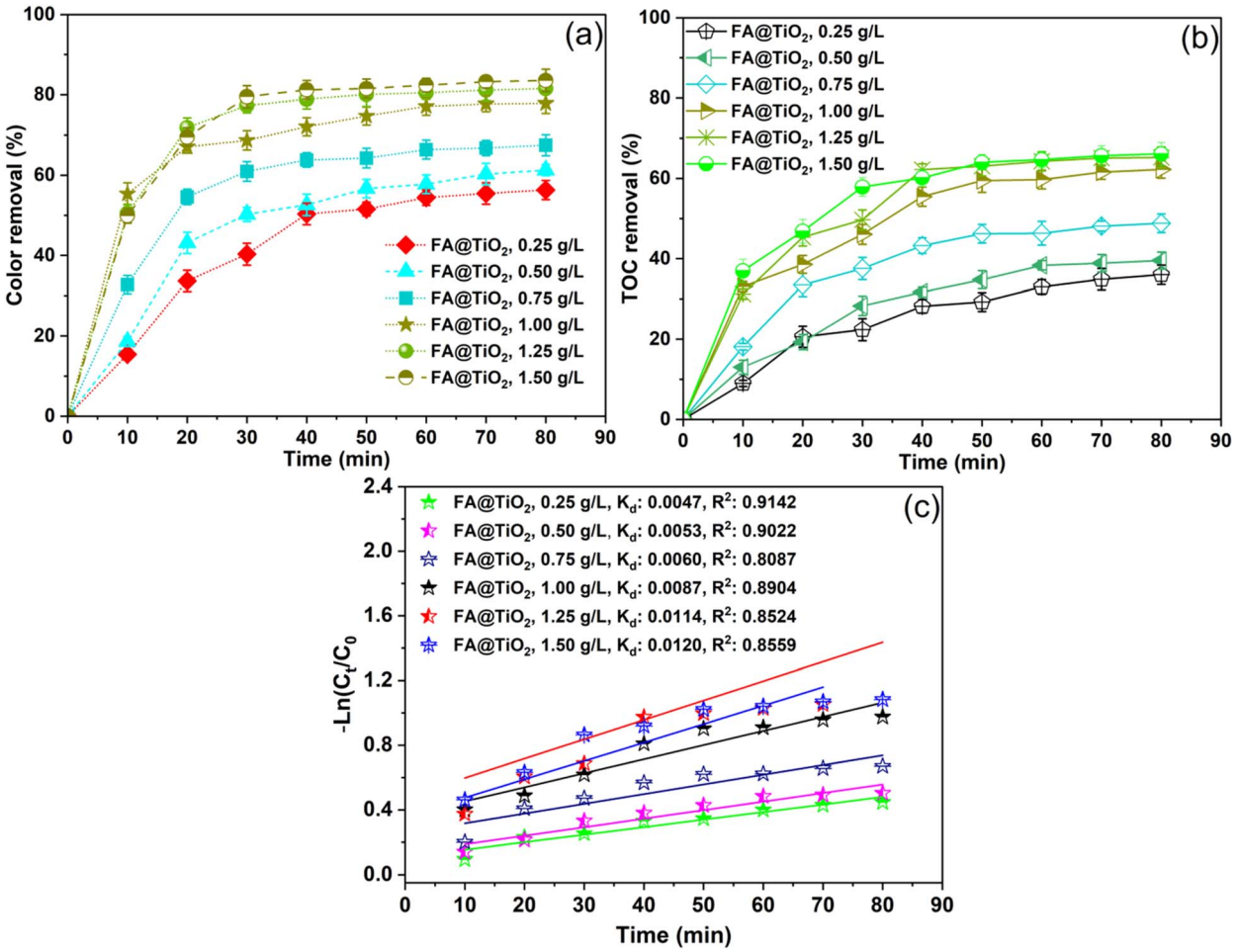

Fig. 6 Influence of catalyst dosage on removal of POCs from landfill leachate (a) color; (b) TOC and (c) pseudo-first-order rate constants by O_3/FA@TiO_2/PMS system at initial TOC concentration of 422 mg L^{-1}; pH of 9.0; PMS dosage of 300 mg L^{-1}, catalyst dosage of 0.25–1.5 g L^{-1} and contact time of 0–80 min.

from 0.9016 to 0.9489). The highest rate constant (k_d = 0.0048 min^{-1}) was recorded at 300 mg L^{-1}, affirming that this dosage provides the optimum balance between effective radical production and minimal self-scavenging effects. Slight deviations in the kinetic constants at 350 mg L^{-1} (k_d = 0.0043 min^{-1}) and 400 mg L^{-1} (k_d = 0.0045 min^{-1}) further substantiate the inference that radical recombination or saturation of active sites on the FA@TiO_2 catalyst may occur at higher PMS concentrations. The pseudo-first-order behavior observed herein aligns with analogous studies involving persulfate activation and other AOP systems.[31,35]

The experimental outcomes strongly reveal that while increasing PMS dosage enhances both color and TOC removal efficiencies, an optimal dosage of 300 mg L^{-1} is identified. At this concentration, the system attains a commendable 61.86% color removal and 38.68% TOC removal, alongside the most favorable kinetic constant, concurrently minimizing the risks of excess PMS usage and secondary pollutant formation. This optimization is not only pivotal for maximizing process efficiency but also bears significant implications for economic and environmental sustainability in practical wastewater treatment applications, particularly in contexts such as landfill leachate management.[34,36]

Effect of FA@TiO_2 dosage

This study was conducted under controlled conditions with an initial TOC concentration of 422 mg L^{-1}, pH = 9.0, a fixed PMS dosage of 300 mg L^{-1}, and varying FA@TiO_2 catalyst dosages ranging from 0.25 to 1.50 g L^{-1} over an 80 min contact period. The performance of the O_3/FA@TiO_2/PMS system was evaluated through three primary metrics: color removal efficiency (%), TOC removal efficiency (%) and the kinetics of TOC degradation (expressed *via* pseudo-first-order rate constants). Similar approaches have been employed in recent works on AOPs for landfill leachate treatment, where the coupling of catalytic ozonation with appropriate catalysts has shown promise in efficiently targeting recalcitrant organic pollutants.[37]

At the lowest dosage of 0.25 g L^{-1}, the color removal efficiency reached 56.30% after 80 min. With an increase in catalyst dosage to 0.50, 0.75, 1.00, 1.25 and 1.50 g L^{-1}, the corresponding color removal efficiencies increased to 61.27%, 67.46%, 77.90%, 81.52% and 83.35%, respectively. The steep

increase observed up to 1.00 g L^{-1} indicates that, at lower dosages, additional active sites on the FA@TiO_2 surface effectively promote the activation of PMS and subsequent ozone decomposition to generate $SO_4^{\bullet-}$ and $^{\bullet}OH$ radicals, which are critical for breaking down chromophoric structures.[38,39] However, the marginal improvements beyond 1.00 g L^{-1} suggest a saturation effect where further enhancement in ROS generation is limited by either catalyst particle aggregation or the finite availability of degradable chromophores in the leachate.[40]

The TOC removal follows a comparable trend. TOC removal efficiency increased significantly from 36.00% at a catalyst dosage of 0.25 g L^{-1} to 61.59% at 1.00 g L^{-1}. At higher dosages (1.25 and 1.50 g L^{-1}), TOC removal reached 65.08% and 65.12%, respectively. This plateauing effect indicates that beyond a certain catalyst concentration, most readily oxidizable organic compounds have been mineralized, while residual substances may require more rigorous treatment conditions. Similar saturation phenomena have been reported in catalytic ozonation studies targeting refractory organic matter, demonstrating the critical balance between catalyst dosage and available substrate concentrations.[41]

A pseudo-first-order kinetic analysis of TOC degradation indicates that the observed rate constants (k_d) for catalyst dosages of 0.25, 0.50, 0.75, 1.00, 1.25 and 1.50 g L^{-1} were 0.0053, 0.0053, 0.0060, 0.0087, 0.0114 and 0.0120 min^{-1}, respectively, with correlation coefficients (R^2) ranging from 0.8087 to 0.9142. Although the highest k_d value of 0.0120 min^{-1} was achieved at 1.50 g L^{-1}, the increase from 1.00 to 1.25 g L^{-1} is relatively marginal. This suggests that while higher dosages enhance the generation rate of reactive oxygen species, potential limitations stemming from particle agglomeration or light scattering effects may inhibit significant further improvements in the degradation kinetics.[37] The pseudo-first-order model applied here is consistent with previous studies on catalytic ozonation kinetics for organic pollutant degradation.[39]

Collectively, the experimental findings demonstrate that FA@TiO_2 dosage significantly influences the efficiency of catalytic ozonation for the degradation of POCs in landfill leachate. Optimal performance, defined by both color and TOC removal efficiencies coupled with favorable degradation kinetics, is achieved at a catalyst dosage of 1.00 g L^{-1}. At this dosage, a color removal efficiency of 77.90% and a TOC removal efficiency of 61.59% were attained, with a rate constant of 0.0087 min^{-1}. The marginal improvements observed beyond this point – from 1.00 g L^{-1} to 1.25 or 1.50 g L^{-1}, which showed only 3.62–5.45% and 3.49–3.53% increases in color and TOC removal, respectively – underscore the presence of a saturation phenomenon likely due to aggregation of catalyst particles or the limited availability of oxidizable substrates. From an economic and practical standpoint, selecting the lower catalyst dosage minimizes material costs and avoids potential side effects such as excessive light scattering while maintaining high treatment efficiency, essential for the scaling up of treatment processes in real landfill leachate applications.[40]

Machine learning model for removal prediction

The performance of four machine learning models – Linear Regression (LR), Artificial Neural Network (ANN), Random Forest (RF), and Support Vector Machine (SVM) – was evaluated for predicting the degradation efficiency of polycyclic organic compounds (POCs) in the ozone-catalytic O_3/FA@TiO_2/PMS system, based on results presented in Fig. 7 and Table 1. Model accuracy and generalization were assessed using key metrics: the coefficient of determination (R^2), Root Mean Square Error (RMSE), and Mean Absolute Error (MAE), calculated for training, test, and overall datasets.

To assess the practical applicability of the models, computational costs were measured as processing times on a system with 8GB RAM and Intel® Core™ i3-10105 CPU @ 3.70 GHz 3.70 GHz. The LR model, using ordinary least squares (lm), required negligible time (<0.1 seconds). The ANN model, trained with grid search over hidden layer sizes (2–20, caret::nnet, see Machine learning modeling and hyperparameter optimization), took 4.07 seconds. The RF model required 16.46 seconds for tuning (random search, caret::rf) and 0.44 seconds for the final model (randomForest), totaling 16.90 seconds. The SVM model needed 11.88 seconds for tuning (random search, caret) and 0.09 seconds for the final model (e1071::svm), totaling 11.97 seconds. These computational costs, alongside performance metrics, enable researchers to select models balancing accuracy and efficiency for similar environmental remediation tasks.

The LR model displayed the weakest predictive capability, evidenced by a test R^2 of 0.891, with an RMSE of 5.606 and an MAE of 4.497. This suggests that LR is ill-suited for capturing the non-linear dynamics of POC degradation within the O_3/FA@TiO_2/PMS system. In contrast, the ANN model excelled, achieving a test R^2 of 0.979, alongside an RMSE of 2.356 and an MAE of 1.786, indicating its proficiency in modeling complex interactions and ensuring robust generalization. The RF model yielded a test set R^2 of 0.93, with an RMSE of 4.924 and an MAE of 3.679, reflecting decent accuracy but a noticeable decline in stability on the test compared to ANN. The SVM model performed strongly with a test R^2 of 0.98, an RMSE of 2.392 and an MAE of 1.948, though its slightly elevated RMSE and MAE values suggest a minor reduction in generalization compared to ANN.

Comparative evaluation underscores that ANN and SVM achieve the highest test R^2 values, nearly equivalent at 0.979 and 0.98, respectively; however, ANN exhibits lower RMSE (2.356) and MAE (1.786) values compared to SVM (RMSE 2.392, MAE 1.948), affirming its appropriateness for modeling the intricate, non-linear degradation processes in the O_3/FA@TiO_2/PMS system. RF offers reasonable accuracy but lacks the stability of ANN, while LR's linear framework proves inadequate for the system's complexity.

ANN's enhanced performance stems from its deep architecture, which adeptly learns intricate patterns and interactions among key variables – ozone concentration, catalyst composition (FA@TiO_2/PMS) and reaction conditions. This is particularly significant in the O_3/FA@TiO_2/PMS system, where photocatalysis and ozonation synergistically drive POC

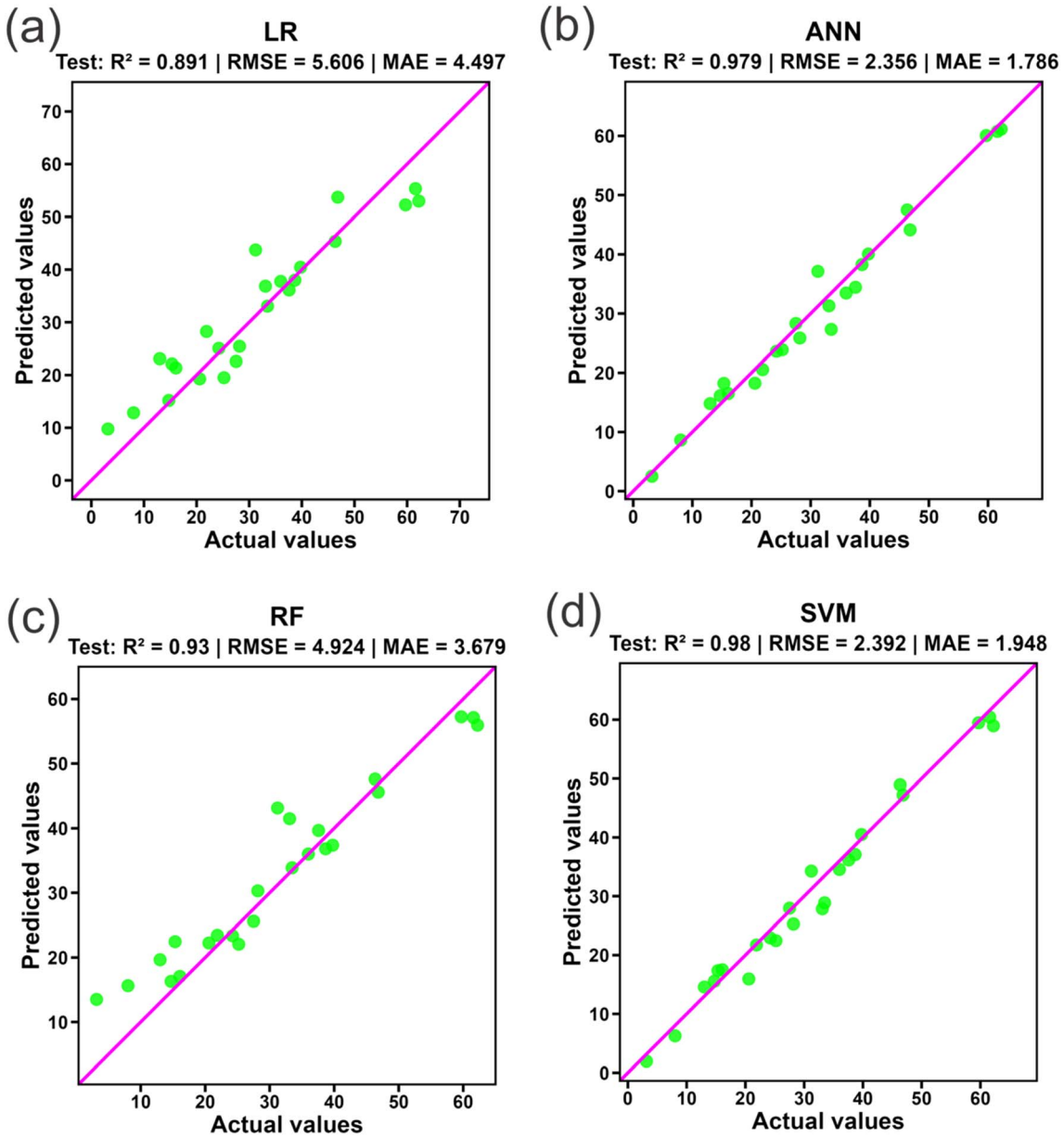

Fig. 7 The prediction of ML models: LR (a); ANN (b); RF (c); SVM (d) for POC degradation efficiency by O_3/FA@TiO_2/PMS system.

Table 1 Hyperparameters and performance of machine learning models

Model	Optimization strategy	Optimal hyperparameters	Test R^2	Test RMSE	Test MAE
LR	None	N/A	0.891	5.606	4.497
ANN	Grid search	Hidden nodes = 4, decay = 0.01, maxit = 50 000	0.979	2.356	1.786
RF	Tune grid search (10-fold CV)	mtry = 2, ntree = 500, nodesize = 5, maxnodes = NULL	0.930	4.924	3.679
SVM	Random search (10-fold CV)	Kernel = polynomial, C = 10, degree = 3, gamma = 0.1, epsilon = 0.1	0.980	2.392	1.948

degradation. The consistent test set performance of ANN highlights its potential for practical applications, especially under variable real-world conditions. These results emphasize the critical role of advanced machine learning, particularly ANN, in enhancing environmental remediation processes. ANN's robust generalization could enable the design of efficient catalytic systems by accurately predicting optimal conditions with reduced experimental effort.

The variable importance analysis, as illustrated in Fig. 8, elucidates the key factors affecting POC degradation efficiency within the O_3/FA@TiO_2/PMS system across different machine learning models. The LR model identifies catalyst dosage (Cat_dos) as the most influential variable, followed by reaction time (Time), with pH and PMS concentration showing comparatively lower importance. This indicates LR's emphasis on catalyst-related parameters, potentially oversimplifying complex interactions due to its linear nature. The ANN model prioritizes reaction time as the dominant factor, closely followed by catalyst dosage, with PMS and pH contributing moderately, highlighting ANN's capacity to model non-linear relationships and temporal-catalytic effects. The RF model ranks catalyst dosage highest, with reaction time as the second key variable, while pH and PMS exert minimal influence, suggesting RF's focus on primary variables may overlook secondary effects. The SVM model designates reaction time as the leading contributor, followed by catalyst dosage, with PMS and pH playing lesser but notable roles, indicating a balanced assessment of process dynamics.

Comparative analysis reveals that reaction time and catalyst dosage consistently rank as the most critical variables across all models, affirming their central role in enhancing POC degradation efficiency. ANN and SVM, leveraging their non-linear modeling strengths, provide a more detailed ranking by acknowledging the contributions of PMS and pH, which LR and RF tend to undervalue. These differing importance rankings reflect the models' varied abilities to capture variable

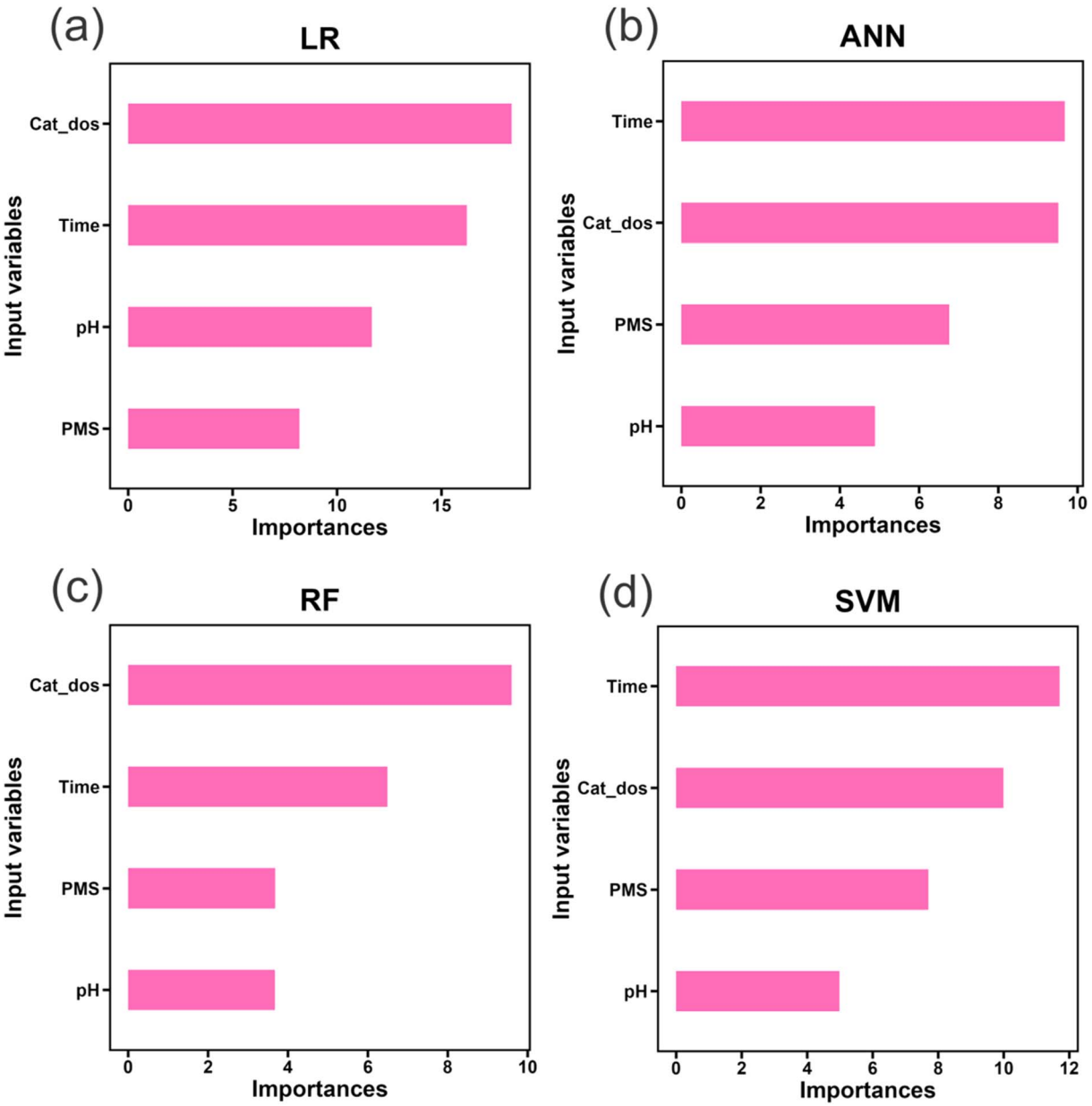

Fig. 8 Importance plot of ML models: LR (a); ANN (b); RF (c); SVM (d) for POC degradation efficiency by O_3/FA@TiO_2/PMS system.

interactions, with ANN and SVM offering a more holistic perspective due to their adaptability to complex systems. These insights suggest that optimizing reaction time and catalyst dosage could substantially improve degradation efficiency, while pH and PMS adjustments may offer additional benefits, particularly when analyzed with advanced models like ANN and SVM. This understanding could inform experimental design and process optimization within the O_3/FA@TiO_2/PMS system, harnessing the capabilities of these machine learning techniques.

Degradation mechanisms

The degradation mechanism of POCs in landfill leachate through the catalytic ozonation process using the FA@TiO_2 composite in the presence of PMS was thoroughly investigated. This study elucidates the synergistic roles of FA@TiO_2, PMS and O_3 in generating ROS responsible for the removal of color and TOC. The influence of radical scavengers (CO_3^{2-} and Cl^-) on the degradation process was also evaluated to identify the dominant reactive species, as presented in Fig. 9. The experimental conditions included an initial TOC concentration of 422 mg L^{-1}, pH of 9.0, PMS dosage of 300 mg L^{-1}, FA@TiO_2 dosage of 1.00 g L^{-1} and a contact time of 80 min.

The FA@TiO_2 composite, synthesized *via* the sol–gel method with a 20% TiO_2 loading, exhibits distinct physicochemical properties that enhance its catalytic performance. As detailed in Characteristics of FA@TiO_2 catalyst, SEM analysis (Fig. 2b1) revealed a uniform distribution of TiO_2 nanoparticles on the porous and rough surface of FA, which originally displayed a heterogeneous structure with aluminosilicate spheres (Fig. 2a1). The EDX analysis (Fig. 2b2) confirmed the successful incorporation of TiO_2, with a titanium content of 5.95 wt% (2.57 atomic%) and an increased oxygen content of 40.39 wt% (43.73 atomic%), reflecting the oxide nature of TiO_2. The XRD patterns (Fig. 3) further validated the presence of the anatase phase of TiO_2 (peaks at $2\theta \approx 25.3°$, 37.8°, 48.0°, 54.0°, and 62.7°) alongside the amorphous FA matrix (broad hump at $2\theta \approx 20$–30°), with crystallite sizes of 15–20 nm, indicating minimal agglomeration and high phase stability.

The FA@TiO_2 composite leverages the complementary properties of FA and TiO_2. Fly ash, rich in metal oxides such as SiO_2, Al_2O_3 and Fe_2O_3 (as evidenced by EDX: Si at 3.12 wt%, Fe

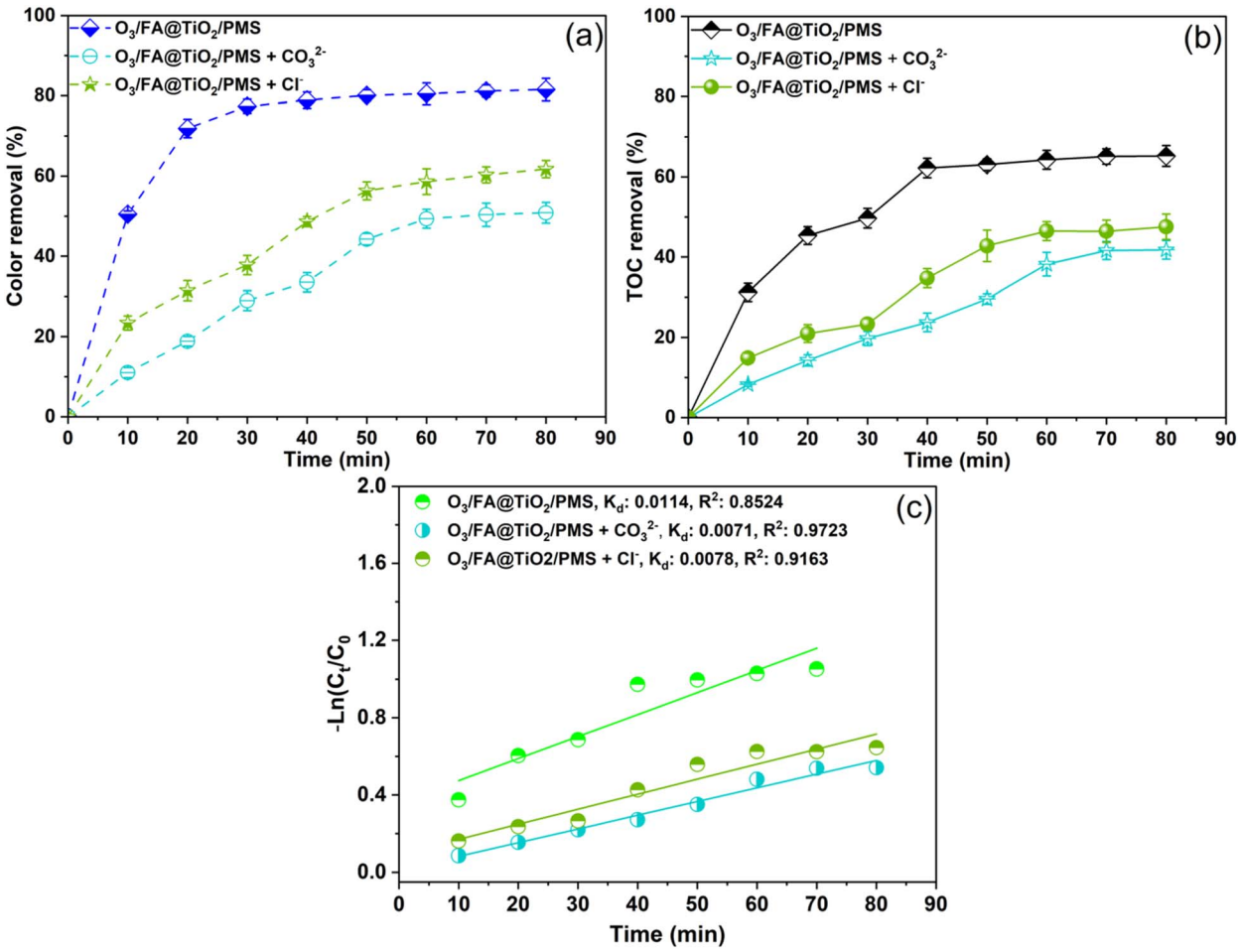

Fig. 9 Influence of scavengers (CO_3^{2-} and Cl^-) on removal of POCs from landfill leachate (a) color; (b) TOC and (c) pseudo-first-order rate constants by O_3/FA@TiO_2/PMS system at initial TOC concentration of 422 mg L^{-1}; pH of 9.0; PMS dosage of 300 mg L^{-1}, catalyst dosage of 1.00 g L^{-1} and contact time of 0–80 min.

at 2.73 wt%), facilitates the decomposition of ozone into hydroxyl radicals (˙OH) through its surface metal sites. TiO_2, with its anatase phase, enhances the generation of ROS by promoting the activation of PMS to produce sulfate radicals ($SO_4^{\cdot-}$) and additional ˙OH radicals. The porous structure of FA (retained in the composite) ensures efficient mass transfer of reactants, while the high surface area of TiO_2 nanoparticles increases the density of catalytic sites, thereby amplifying the overall oxidative capacity of the O_3/FA@TiO_2/PMS system.

Fig. 10 schematically illustrates the mechanism underlying the degradation of color and TOC in landfill leachate. The diagram delineates the mechanism of pollutant breakdown, providing a comprehensive depiction of the processes involved. Subsequent analysis elucidates the fundamental principles that govern these degradation pathways and their corresponding influence on the treatment efficiency. Moreover, the empirical observations derived from this study substantiate the proposed mechanism, thereby offering valuable insights into its practical applicability in leachate remediation.

Ozone decomposition and ROS generation by FA@TiO_2: upon introduction into the reaction system, O_3 interacts with the FA@TiO_2 surface, where the metal oxides present in FA (*e.g.*, Fe_2O_3) and the catalytic anatase TiO_2 sites drive the decomposition of O_3 into hydroxyl (˙OH) radicals *via* the following reactions:

$$O_3 + FA@TiO_2 \rightarrow O_2 + O^{-\cdot} \text{ (surface-bound)}$$

$$O^- + H_2O \rightarrow {}^{\cdot}OH + OH^-$$

Under alkaline conditions (pH 9.0), the deprotonation of surface hydroxyl groups on TiO_2 further expedites this electrophilic attack mechanism by O_3. This behavior aligns with observations in AOPs applied to landfill leachate.[42]

PMS activation by FA@TiO_2: PMS is activated by the FA@TiO_2 composite to generate $SO_4^{\cdot-}$ and ˙OH radicals. The Fe_2O_3 in FA and the TiO_2 nanoparticles play a synergistic role in this activation. The Fe^{3+}/Fe^{2+} redox cycle on the FA surface catalyzes PMS decomposition:

$$Fe^{3+} + HSO_5^- \rightarrow Fe^{2+} + SO_5^{\cdot-} + H^+$$

$$Fe^{2+} + HSO_5^- \rightarrow Fe^{3+} + SO_4^{\cdot-} + OH^-$$

Simultaneously, TiO_2 activates PMS through its surface Ti^{4+} sites, which can be reduced to Ti^{3+}, facilitating the generation of $SO_4^{\cdot-}$:

$$Ti^{4+} + HSO_5^- \rightarrow Ti^{3+} + SO_5^{\cdot-} + H^+$$

$$Ti^{3+} + HSO_5^- \rightarrow Ti^{4+} + SO_4^{\cdot-} + OH^-$$

The $SO_4^{\cdot-}$ radicals can further react with water or OH^- to produce ˙OH:

$$SO_4^{\cdot-} + H_2O \rightarrow SO_4^{2-} + {}^{\cdot}OH + H^+$$

$$SO_4^{\cdot-} + OH^- \rightarrow SO_4^{2-} + {}^{\cdot}OH$$

These reaction pathways augment ROS production, which has similarly been reported in catalytic ozonation studies applied to complex wastewater matrices.[37,43]

Synergistic interaction of O_3 and PMS: the presence of PMS enhances the decomposition of O_3 by reacting with O_3-derived species, leading to the formation of additional ROS:

$$O_3 + HSO_5^- \rightarrow SO_5^{\cdot-} + O_2 + OH^-$$

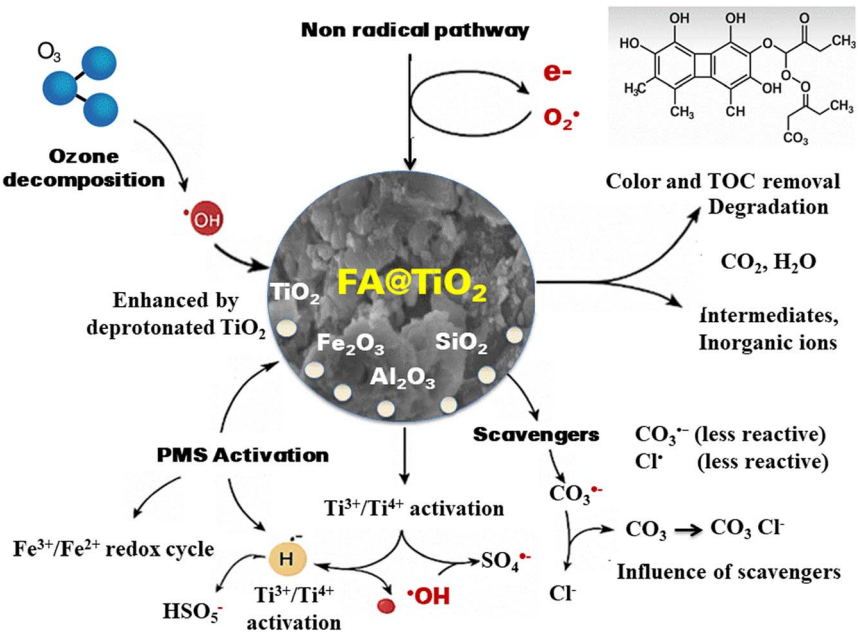

Fig. 10 Proposed mechanism for POC degradation from landfill leachate by O_3/FA@TiO_2/PMS system.

$$SO_5^{\cdot-} + H_2O \rightarrow SO_4^{\cdot-} + {}^{\cdot}OH + H^+$$

This synergistic effect significantly increases the concentration of ROS, thereby enhancing the oxidative degradation of POCs.

Degradation of color and TOC: the generated $^{\cdot}OH$ and $SO_4^{\cdot-}$ radicals are highly reactive and non-selective, attacking the chromophoric groups (*e.g.*, conjugated double bonds in humic substances) responsible for the color of leachate, as well as the organic carbon backbone. The color removal process involves the cleavage of chromophores, leading to decolorization, while TOC removal entails the mineralization of organic compounds into CO_2 and H_2O. For instance, humic substances, which constitute up to 60% of organic matter in aged leachate,[44] were broken down through the following generalized pathway:

$$\text{POCs} + {}^{\cdot}OH/SO_4^{\cdot-} \rightarrow \text{intermediates} \rightarrow CO_2 + H_2O + \text{inorganic ions}$$

The high color removal efficiency (81.52% at 80 min with 1.00 g per L FA@TiO_2, as shown in Fig. 6a) indicates rapid cleavage of chromophoric structures, while the TOC removal efficiency (65.23% under optimal conditions with O_3/FA@TiO_2/PMS system, as shown in Fig. 6b) reflects substantial mineralization of organic carbon.

Beside, SiO_2 and Al_2O_3 in FA substantively contribute to the formation of additional surface hydroxyl groups, which in turn enhance the adsorption of O_3 and POCs. This adsorption facilitates the catalytic decomposition of O_3 into $^{\cdot}OH$ radicals. In particular, Al_2O_3 serves as a Lewis acid site that promotes stronger interactions between O_3 and the catalyst surface, thereby augmenting the generation of ROS essential for POC degradation. Moreover, the inherent metal oxides in FA, notably SiO_2 and Al_2O_3, are crucial in catalyzing the decomposition of O_3 as well as activating PMS, as highlighted by their documented functional roles in AOPs.

Influence of radical scavengers (CO_3^{2-} and Cl^-). The role of $^{\cdot}OH$ and $SO_4^{\cdot-}$ radicals in the degradation process was further elucidated by introducing CO_3^{2-} and Cl^- as radical scavengers, as shown in Fig. 9. These anions are known to react with $^{\cdot}OH$ and $SO_4^{\cdot-}$, thereby inhibiting their availability for POC degradation.

Color removal efficiency (Fig. 9a): in the absence of scavengers, the O_3/FA@TiO_2/PMS system achieved a color removal efficiency of 81.52% after 80 min. The addition of CO_3^{2-} reduced this efficiency to 50.84%, while Cl^- further decreased it to 61.73%. CO_3^{2-} reacts with $^{\cdot}OH$ and $SO_4^{\cdot-}$ to form less reactive carbonate radicals ($CO_3^{\cdot-}$):

$$CO_3^{2-} + {}^{\cdot}OH \rightarrow CO_3^{\cdot-} + OH^-$$

$$CO_3^{2-} + SO_4^{\cdot-} \rightarrow CO_3^{\cdot-} + SO_4^{2-}$$

These reactions significantly reduce the availability of $^{\cdot}OH$ and $SO_4^{\cdot-}$, leading to a 30.68% decrease in color removal efficiency. Cl^-, on the other hand, reacts with $^{\cdot}OH$ and $SO_4^{\cdot-}$ to form chlorine radicals ($Cl^{\cdot}$) and other less reactive species:

$$Cl^- + {}^{\cdot}OH \rightarrow ClOH^{\cdot-}$$

$$ClOH^{\cdot-} + H^+ \rightarrow Cl^{\cdot} + H_2O$$

$$Cl^- + SO_4^{\cdot-} \rightarrow Cl^{\cdot} + SO_4^{2-}$$

The Cl^- scavenger caused a 19.79% reduction in color removal efficiency, indicating that while both $^{\cdot}OH$ and $SO_4^{\cdot-}$ are critical, the system is more sensitive to the scavenging of $^{\cdot}OH$ by CO_3^{2-}.

TOC removal efficiency (Fig. 9b): the TOC removal efficiency followed a similar trend, decreasing from 65.23% (without scavengers) to 41.78% with CO_3^{2-} and 47.53% with Cl^- after 80 min. The 23.45% reduction with CO_3^{2-} and 17.70% reduction with Cl^- further confirm the dominant role of $^{\cdot}OH$ in the mineralization process, as CO_3^{2-} more effectively scavenges $^{\cdot}OH$ compared to Cl^-. The pseudo-first-order rate constants (Fig. 9c) also decreased from 0.0087 min^{-1} (without scavengers) to 0.0054 min^{-1} with CO_3^{2-} and 0.0064 min^{-1} with Cl^-, reflecting a slower degradation rate due to reduced ROS availability.

The results indicate that both $^{\cdot}OH$ and $SO_4^{\cdot-}$ are pivotal in the degradation of POCs, with $^{\cdot}OH$ playing a more dominant role in the mineralization of organic carbon, as evidenced by the greater inhibition effect of CO_3^{2-} compared to Cl^-. The FA@TiO_2 composite enhances the generation of these radicals through its dual catalytic action: the FA component facilitates ozone decomposition, while TiO_2 activates PMS, leading to a synergistic increase in ROS production.

The color removal process primarily involves the oxidative cleavage of chromophoric groups, which occurs rapidly due to the high reactivity of $^{\cdot}OH$ and $SO_4^{\cdot-}$ with conjugated systems. In contrast, TOC removal requires the complete mineralization of organic carbon, a process that is more dependent on $^{\cdot}OH$ due to its non-selective nature and higher oxidation potential (E_o = 2.8 V) compared to $SO_4^{\cdot-}$ (E_o = 2.5–3.1 V).[45] The plateauing of TOC removal efficiency at higher FA@TiO_2 dosages (Fig. 6b) and PMS dosage (Fig. 5b) suggests that the remaining organic fractions are recalcitrant, likely consisting of smaller, more stable intermediates that resist further oxidation under the given conditions. These findings align with literature reports highlighting the critical influence of competing anions on the performance of AOP systems in leachate treatment applications[42]

The presence of scavengers highlights the sensitivity of the system to environmental factors such as coexisting anions, which are common in landfill leachate. The greater inhibition by CO_3^{2-} suggests that strategies to mitigate carbonate interference (*e.g.*, pH adjustment or pre-treatment to remove CO_3^{2-}) could further enhance the system's performance. Moreover, the alkaline pH (9.0) used in this study favors the generation of $^{\cdot}OH$, as confirmed by the pH effect study (Characteristics of FA@TiO_2 catalyst), where TOC removal increased from 27.48% at pH 7 to

38.19% at pH 9. This is consistent with the deprotonation of PMS and organic compounds under alkaline conditions, facilitating radical-mediated oxidation.

Reusability of catalyst

The reusability performance of the FA@TiO_2 catalyst in the degradation of POCs in landfill leachate was evaluated in the O_3/FA@TiO_2/PMS system under controlled conditions (Fig. 11). Initial findings indicate that the catalyst exhibits high activity, with a first-cycle performance yielding a color removal efficiency of 85.96% and a TOC removal efficiency of 66.33%. However, over five successive cycles, both color and TOC removal efficiencies decreased, reaching 78.32% and 51.71% in cycle two, 75.55% and 45.00% in cycle three, 68.12% and 43.16% in cycle four, and finally 67.52% and 40.62% in cycle five.

This decline in catalytic performance can be attributed to several interrelated factors. First, potential leaching of active catalytic sites from the FA@TiO_2 surface under prolonged exposure to oxidative conditions is a plausible mechanism, as similar phenomena have been observed in other PMS-activated systems. Second, the accumulation of intermediate byproducts may lead to blocking or poisoning of the active sites, thereby inhibiting further catalytic activity. Comparable issues of surface fouling leading to decreased activity over multiple cycles have been documented in studies addressing PMS activation for pollutant degradation. Third, the oxidative environment inherent to the O_3/PMS system could induce partial deactivation of the catalyst, a challenge noted in studies involving TiO_2-based catalysts.

Despite the observed decline in performance, the FA@TiO_2 catalyst retained a moderate level of activity after five cycles, with the color removal efficiency remaining above 67% and the TOC removal efficiency staying above 40%. These results underscore the feasibility of employing the FA@TiO_2 catalyst for practical applications in landfill leachate treatment, while also highlighting the need for further optimization. Strategies such as surface modification or the implementation of regeneration protocols may enhance the stability and longevity of the catalyst in advanced oxidation processes. Recent literature supports that modifications and regeneration techniques can improve catalytic robustness and operational durability.

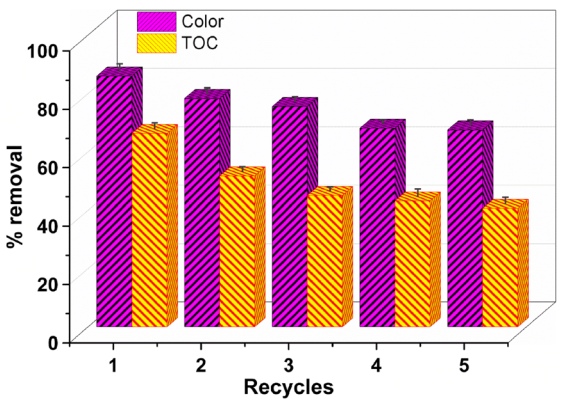

Fig. 11 The reusability of the FA@TiO_2 catalyst in the degradation of POCs during landfill leachate treatment using the O_3/FA@TiO_2/PMS system. Experimental conditions: TOC concentration of 432 mg L^{-1}; pH of 9.0; PMS dosage of 300 mg L^{-1}, catalyst dosage of 1.00 g L^{-1} and contact time of 0–80 min.

Conclusions

This study demonstrates the efficacy of a hybrid O_3/FA@TiO_2/PMS system for treating landfill leachate, achieving significant degradation of persistent organic compounds under optimized conditions. The FA@TiO_2 composite, with an optimal TiO_2 loading of 20%, exhibited superior performance, attaining 77.90% color removal and 61.59% TOC removal at pH 9, PMS dosage of 300 mg L^{-1}, and catalyst dosage of 1.00 g L^{-1} after 80 min. These conditions yielded a pseudo-first-order rate constant of 0.0087 min^{-1}, reflecting efficient ROS generation, primarily $^{\bullet}OH$ and $SO_4^{\bullet-}$ radicals, with OH identified as the dominant species for TOC mineralization. The system's synergy stems from FA's metal oxides (*e.g.*, SiO_2, Al_2O_3, Fe_2O_3) and TiO_2's anatase phase, enhancing ozone decomposition and PMS activation. Reusability tests over five cycles showed a decline to 67.52% color and 40.62% TOC removal, suggesting practical applicability despite challenges like site leaching and byproduct accumulation. These findings highlight the potential of FA@TiO_2 as a cost-effective, sustainable catalyst, repurposing industrial waste for environmental remediation. The Artificial Neural Network's exceptional predictive performance underscores its potential for optimizing complex environmental remediation processes, particularly in modeling non-linear POC degradation dynamics in the O_3/FA@TiO_2/PMS system.

Author contributions

Thi Cuc Luu: funding acquisition, investigation; Thuy Linh Vi, Hoang Nguyen: conceptualization, data curation; Thi Bich Lien Nguyen, Thu Huong Nguyen: formal analysis; Thi Cuc Luu, Trung Kien Hoang, Thi Hanh Dam, Duc Hien Lu, A Dia Thao: resources, software; Thi Cuc Luu, Huu-Tap Van, Thi Bich Lien Nguyen: writing – original draft; Huu-Tap Van, Lan Huong Nguyen: methodology; Van Hung Hoang and Huu-Tap Van: writing – review & editing.

Conflicts of interest

The authors declare that they have no known competing financial interests or personal relationships that could have appeared to influence the work reported in this paper.

Data availability

Data associated with this study has not been deposited into a publicly available repository. Data will be made available on request.

The SI is presented *via* a GitHub repository (**https://github.com/vanhuutap/Landfill-leachate-removal-by-O3**). See DOI: **https://doi.org/10.1039/d5ra04088d**.

Acknowledgements

This research is funded by Ministry of Education and Training (MOET) under grant number B2024-TNA-06.

References

1 C. Costa, M. L. Pinedo and B. D. Riascos, *Sustainability*, 2025, **17**, 481.
2 V. Gunarathne, A. J. Phillips, A. Zanoletti, A. U. Rajapaksha, M. Vithanage, F. Di Maria, A. Pivato, E. Korzeniewska and E. Bontempi, *Sci. Total Environ.*, 2024, **912**, 169026.
3 C. E. W. Steinberg, N. Saul, K. Pietsch, T. Meinelt, S. Rienau and R. Menzel, *Ann. Environ. Sci.*, 2007, **1**, 81–90.
4 M. Morozesk, M. M. Bonomo, I. da C. Souza, L. D. Rocha, I. D. Duarte, I. O. Martins, L. B. Dobbss, M. T. W. D. Carneiro, M. N. Fernandes and S. T. Matsumoto, *Chemosphere*, 2017, **184**, 309–317.
5 B. Gao, X. Yang, E. A. Dasi, T. Lam, M. E. Arias and S. J. Ergas, *J. Chem. Technol. Biotechnol.*, 2022, **97**, 759–770.
6 E. Gripa, J. C. Campos and F. V da Fonseca, *J. Water Process Eng.*, 2021, **43**, 102264.
7 Z. Guo, Y. Zhang, H. Jia, J. Guo, X. Meng and J. Wang, *Sci. Total Environ.*, 2022, **806**, 150529.
8 A. Ali, C. Junkui, S. Weihua and D. Yang, *J. Environ. Eng.*, 2022, **148**, 4022046.
9 S. N. F. Zakaria, N. Bolong, I. Saad and H. A. Aziz, *IOP Conf. Ser.:Mater. Sci. Eng.*, 2022, **1229**, 12015.
10 S. S. Moersidik, L. Annasari and R. Nugroho, *International Journal of Technology*, 2021, **12**, 78.
11 S. N. F. Zakaria, H. A. Aziz, M. Mohamad, H. M. Mohamad and M. F. Sulaiman, *Water Environ. Res.*, 2023, **95**, e10941.
12 C. Ma, P. Ma, Z. He and M. Xiao, *Toxics*, 2022, **10**, e505.
13 M. A. Sari, J. Oppenheimer, K. Robinson, J. E. Drewes, A. N. Pisarenko, V. Sundaram and J. G. Jacangelo, *AWWA Water Sci.*, 2020, **2**, e1193.
14 A. J. Kadem, Z. M. Tan, N. M. Suntharam, S. Pung and S. Ramakrishnan, *Bull. Chem. React. Eng. Catal.*, 2023, **18**, 506–520.
15 T. Dontsova, A. Kutuzova, K. O. Bila, S. Kyrii, I. Kosogina and D. O. Nechyporuk, *J. Nanomater.*, 2020, **2020**, 1–13.
16 Y. Chen, R. Chen, X. Chang, J. Yan, Y. Gu, S. Xi, P. Sun and X. Dong, *Water*, 2023, **15**, 3801.
17 O. Purba, R. Yanda, A. Munandar, F. C. Alam and T. Taher, *IOP Conf. Ser. Earth Environ. Sci.*, 2024, **1317**, 12023.
18 A. Hassani, J. Scaria, F. Ghanbari and P. V Nidheesh, *Environ. Res.*, 2023, **217**, 114789.
19 M. R. R. Kooh, R. Thotagamuge, Y. F. Chou Chau, A. H. Mahadi and C. M. Lim, *J. Taiwan Inst. Chem. Eng.*, 2022, **132**, 104134.
20 R. T. Schossler, S. Ojo, Z. Jiang, J. Hu and X. Yu, *Sci. Rep.*, 2024, **14**, 1–15.
21 E. Vakarelska, M. Nedyalkova, M. Vasighi and V. Simeonov, *Chemosphere*, 2022, **287**, 132189.
22 Z. Liu, J. Wu, K. Li, C. Song and X. Guo, *Ind. Eng. Chem. Res.*, 2024, **63**, 9082–9092.
23 X. Yue, Y. Wang, Z. Jiang, B. Deng and Z. Jiang, *ChemSusChem*, 2024, **17**, e202400254.
24 M. Kumari and M. Pulimi, *ACS Omega*, 2023, **8**, 34262–34280.
25 S. S. Alterary and N. H. Marei, *J. King Saud Univ., Sci.*, 2021, **33**, 101536.
26 W. Tao, F. Fei and W. Yue-Chuan, *Polym. Bull.*, 2006, **56**, 413–426.
27 P. Ribeiro, V. Freitas, K. Machry, A. Muniz and G. Rosa, *Environ. Sci. Pollut. Res.*, 2019, **26**, 28603–28613.
28 K. Wang, Y. Zhuo, J. Chen, D. Gao, Y. Ren, C. Wang and Z. Qi, *RSC Adv.*, 2020, **10**, 43592–43598.
29 J. Rodríguez-Chueca, E. Alonso and D. N. Singh, *Int. J. Environ. Res. Public Health*, 2019, **16**, 198.
30 M. A. Zazouli, Z. Yousefi, E. Babanezhad, R. A. Mohammadpour and A. Ala, *Environ. Health Eng. Manage. J.*, 2024, **11**, 105–125.
31 A. Enfiyeci and D. İ. Çifçi, *J. Chem. Technol. Biotechnol.*, 2024, **100**, 466–476.
32 F. Ung-Medina, U. Caudillo-Flores, J. C. Correa-González, R. Maya-Yescas, M. del C. Chávez-Parga and J. A. Cortés, *Environ. Prog. Sustainable Energy*, 2017, **36**, 1083–1088.
33 A. Asghar, N. Ramzan, B. ul Jamal, M. Maqsood, B. Sajjadi and W. Chen, *Water Environ. J.*, 2019, **34**, 523–535.
34 A. Mondala, R. Hernández, W. T. French, L. A. Estévez, M. W. Meckes, M. Trillo and J. A. Hall, *Environ. Prog. Sustainable Energy*, 2010, **30**, 666–674.
35 S. Jorfi and Z. Ghaedrahmat, *Environ. Prog. Sustainable Energy*, 2020, **40**, e13531.
36 Y. Li, X. Liu, Q. Zhang, B. Wang, C. Yu, H. U. Rashid, Y. Xu, L. Ma and F. Lai, *Molecules*, 2018, **23**, 2816.
37 R. P. de Brito, H. J. I. Filho, L. G. Aguiar, M. A. K. de Alcântara, A. A. G. Siqueira and P. C. M. Da Rós, *Ind. Eng. Chem. Res.*, 2019, **58**, 9855–9863.
38 H. T. Van, V. H. Hoang, T. C. Luu, T. K. Linh, L. T. Q. Nga, G. S. I. J. Marcaida and P. T. Tho, *RSC Adv.*, 2023, **13**, 28753–28766.
39 X. Tang, Y. Zhang, W. Li, J. Geng, H. Ren and K. Xu, *Sci. Rep.*, 2021, **11**, 8748.
40 Y. Wang and K. Chen, *Int. J. Environ. Res. Public Health*, 2014, **11**, 9325–9344.
41 B. Gao, H. Zhang, F. Wang, X. Xiong, K. Tian, Y. Sun and T. Yu, *Catalysts*, 2019, **9**, 241.
42 A. P. J. Scandelai, E. Sloboda Rigobello, B. L. C. de Oliveira and C. R. G. Tavares, *Environ. Technol.*, 2019, **40**, 730–741.
43 S. Kow, M. R. Fahmi, C. Z. A. Abidin and O. Soon-An, *Water Environ. Res.*, 2016, **88**, 2047–2058.
44 Z. Yuan, C. He, Q. Shi, C. Xu, L. I. Zhen-shan, C. Wang, H. Zhao and J. Ni, *Environ. Sci. Technol.*, 2017, **51**, 8110–8118.
45 L. H. Nguyen, X. H. Nguyen, V. L. Nguyen, V. T. Pham, V. N. Thai, T. Le Luu, V. H. Tap and H. Nghiem Le, *J. Environ. Chem. Eng.*, 2023, **11**, 110076.